Beyond Conventional Treatments: Unveiling the Promising Role of Chalcone Derivatives in Overcoming Ovarian Cancer

by

İdil Su Canıtez

A Dissertation Submitted to the
Graduate School of Health Sciences
in Partial Fulfillment of the Requirements for
the Degree of
Master of Science

in

Cellular and Molecular Medicine Program

August 3, 2023

Beyond Conventional Treatments: Unveiling the Promising Role of Chalcone Derivatives in Overcoming Ovarian Cancer

Koç University

Graduate School of Health Sciences

This is to certify that I have examined this copy of a master's thesis by

İdil Su Canıtez

and have found that it is complete and satisfactory in all respects,
and that any and all revisions required by the final
examining committee have been made.

Committee Members:

Assist. Prof. İrem Durmaz Şahin (Advisor)

Assist. Prof. Ebru Bilget Güven

Assist. Prof. Zelal Adıgüzel

Date: August 3, 2023

This thesis is dedicated to my parents.

For their endless love, support, and encouragement

ABSTRACT

BEYOND CONVENTIONAL TREATMENTS: UNVEILING THE PROMISING ROLE OF CHALCONE DERIVATIVES IN OVERCOMING OVARIAN CANCER

İdil Su Canıtez

Master of Science in

Cellular and Molecular Medicine Master's with Thesis Program

August 3, 2023

Epithelial ovarian cancer is an aggressive type of cancer in people with ovaries causing significant mortality rates worldwide, and remains incurable especially in advanced stages due to chemoresistance and drug-associated side effects. To address this issue, identifying novel chemotherapeutic agents showing low side effects and enhanced anti-cancer activity is crucial. In this thesis, a collection of chalcone analogues were examined to evaluate their potential as anti-cancer agents against ovarian cancer cells. The specific aim of this study was to identify and characterize novel agents that could overcome chemoresistance and improve the efficacy of ovarian cancer treatment. To achieve this, NCI-SRB assay was performed on four distinct cell lines, including both ovarian cancer and non-tumorigenic cells, to investigate the potential cytotoxic activity of 16 novel chalcone derivatives. Through the application of the NCI-SRB assay, chalcone derivatives exhibiting promising efficacy against ovarian cancer cells were selected for further analysis. To further characterize the underlying cell death mechanisms, various experimental approaches including clonogenic assay, MUSE Annexin-V assay, PI staining, Caspase-3/7 assay, and western blot analysis were employed. It was revealed that out of the 16 chalcone compounds tested, three exhibited promising activity against ovarian cancer cells, having low IC_{50} concentrations. After further investigating the cellular pathways which these compounds targets, these derivatives were also found to induce apoptotic cell death, cause DNA damage through phosphorylation of H2AX, and cause a cell cycle arrest in ovarian cancer cells leading to SubG1 increase. Furthermore, the anti-proliferative activities of selected chalcone compounds were confirmed both *ex vivo* and *in vitro* using primary cell cultures isolated from tumor samples of ovarian cancer patients, and chemoresistant ovarian cancer cells established in our lab, which demonstrated a noticeable decrease in cell viability. Overall, this thesis highlights the potential of the newly identified chalcone compounds as promising molecules in the treatment of ovarian cancer. These promising results warrant further investigation and development of these chalcones as therapeutic agents for ovarian cancer.

ÖZET

GELENEKSEL TEDAVİLERİN ÖTESİNDE: KALKON TÜREVLERİNİN YUMURTALIK KANSERİ TEDAVİSİNDEKİ UMUT VEREN ROLÜNÜN ARAŞTIRILMASI

İdil Su Canıtez

Hücresel ve Moleküler Tıp Tezli Yüksek Lisans Programı,

Yüksek Lisans

Ağustos 3, 2023

Epitelyal yumurtalık kanseri, kadınlarda yaygın bir kanser türü olup dünya genelinde önemli ölüm oranlarına neden olmaktadır ve özellikle ileri evrelerde kemoresistans ve ilaçla ilişkili yan etkiler nedeniyle tedavi edilemez durumdadır. Bu sorunu çözmek için, daha az yan etkiye ve gelişmiş anti-kanser aktivitesine sahip yeni kemoterapötik ajanların tanımlanması çok önemlidir. Bu tezde, yumurtalık kanseri hücrelerine karşı anti-kanser etki potansiyellerini değerlendirmek amacıyla yeni-sentez kalkon molekülleri incelenmiştir. Bu çalışmanın asıl amacı, kemorezistansa karşı koyabilen ve yumurtalık kanseri tedavisinin etkinliğini arttırabilen yeni ajanların belirlenmesi, karakterizasyonu ve bu ajanların etki mekanizmalarının aydınlatılmasıdır. Bu amaçla, 16 yeni kalkon türevinin potansiyel sitotoksik aktivitesini araştırmak için hem yumurtalık kanseri hem de tümörijenik olmayan hücreler dahil olmak üzere dört farklı hücre hattı üzerinde NCI-SRB testi yapıldı. NCI-SRB testinin uygulanmasıyla, yumurtalık kanseri hücrelerine karşı etkili olduğu belirlenen kalkon molekülleri ileri analiz için seçildi. Altta yatan hücre ölüm mekanizmalarını aydınlatmak amacıyla klonojenik yöntem, PI boyama, MUSE Annexin-V boyama, Caspase-3/7 tahlili ve western blot analizi dahil olmak üzere çeşitli deneysel yöntemler kullanıldı. Test edilen 16 kalkon molekülünden üçünün yumurtalık kanseri hücrelerine karşı düşük IC_{50} değerleri ile güçlü sitotoksik aktivite gösterdiği ortaya çıkmıştır. Bu moleküllerin etki şekli daha fazla araştırıldıktan sonra, moleküllerin apoptotik hücre ölümüne neden olduğu, H2AX fosforilasyonu yoluyla DNA hasarına neden olduğu ve yumurtalık kanseri hücrelerinde SubG1 artışına neden olarak hücre döngüsünü etkiledikleri bulundu. Ayrıca, seçilen kalkon moleküllerinin anti-proliferatif aktiviteleri, yüksek dereceli seröz yumurtalık kanseri hastalarının tümör dokusundan elde edilen *ex vivo* primer hücre kültürleri ile birlikte labımızda oluşturulmuş kemorezistans gösteren *in vitro* yumurtalık kanseri modellerinde doğrulanmış ve moleküller hücre canlılığında belirgin bir azalmaya neden olmuştur. Sonuç olarak, bu tez, yeni-sentez kalkon moleküllerinin yumurtalık kanseri tedavisinde umut vaat eden kemoterapötik ajanlar olarak potansiyelini vurgulamaktadır. Bu umut verici sonuçlar, yumurtalık kanseri için potansiyel terapötik ajanlar olarak kalkon moleküllerinin daha fazla araştırılmasını ve geliştirilmesini gerektirmektedir.

AKNOWLEDGEMENTS

First of all, I would like to express my sincere appreciation to my supervisor Dr. İrem Durmaz Şahin for giving me the opportunity to be a member of her lab and for giving me all the support and encouragement throughout this project. She was not only a supervisor for me but also a great mentor who believed in me and gave her invaluable support any time I might need.

I also would like to thank my IDS lab members; Elif Merve Aydın, Deren Demirel, and Gizem Yılmaz Demir for their priceless support and for sharing their knowledge with me. They all created the best working environment full of laughter. I thank them for everything they provided to me both scientifically and personally, from the scientific discussions we had on the balcony to the moments we laughed together.

I would like to send my special thanks to Cem Selçuk for giving me full of support whenever I needed it. He was with me at the finest and hardest times throughout this project.

Lastly, I would like to thank my beloved parents and family members for their endless support and for being always there for me. They gave me the life every child deserves and I dedicate this thesis to them.

August, 2023 İdil Su Canıtez

TABLE OF CONTENTS

LIST OF TABLES

LIST OF FIGURES

ABBREVIATIONS

AKT	Protein kinase B
Amp B	Amphotericin B
Bax	Bcl-2-associated X protein
BCA	Bicinchoninic acid
BRCA	BReast CAncer gene
CI	Combination index
CO_2	Carbon dioxide
DAPI	4',6-diamino-2-phenylindole
ddH_2O	Doubled distilled water
DMEM:F12	Dulbecco's Modified Eagle Medium/Nutrient Mixture F-12
DMSO	Dimethyl Sulfoxide
DNA	Deoxyribonucleic acid
DPBS	Dulbecco's Phosphate Buffered Saline
E-cadherin	Epithelial-cadherin
ECL	Enhanced chemiluminescence
EDTA	Ethylenediaminetetraacetic acid
EGF	Epidermal growth factor
EOC	Epithelial ovarian cancer
EMT	Epithelial-mesenchymal transition
ERK	Extracellular signal-regulated kinase
FBS	Fetal bovine serum
FGF	Fibroblast growth factor
H2AX	Histone family member X
G	Gram
G0/G1	Gap 0 phase/Gap 1 phase
G2/M	Gap 2 phase/Mitosis
HBSS	Hanks' Balanced Salt Solution
HCC	Hepatocellular carcinoma
HGSOC	High-grade serous ovarian cancer
HR	Homologous recombination
IC_{50}	Half-maximal inhibitory concentration

IF	Immunofluorescence
ISL	Isoliquiritienin
kDa	kilodaltons
MDR	Multidrug resistance
µg	Microgram
µl	Microliter
uM	Micromolar
ml	Milliliter
NACI	Sodium Chloride
NaN_3	Sodium azide
N-cadherin	Neural cadherin
NFκB	Nuclear factor kappa B
NOD/SCID	Nonobese diabetic/severe combined immunodeficiency
N/A	Not available
OC	Ovarian cancer
p-Akt	Phosphorylated protein kinase B
PARP-1	Poly (ADP-ribose) polymerase 1
PhosSTOP	Phosphatase inhibitors
PI	Propidium Iodide
PIC	Protease inhibitor cocktail
PI3K	Phosphoinositide 3-kinase
P21	Cyclin-dependent kinase inhibitor 1
P53	Tumor protein 53
p-p53	Phosphorylated tumor protein 53
PS	Phosphatidlyserine
P/S	Penicillin/Streptomycin
PVDF	Polyvinylidene fluoride
Ras	Rat sarcoma virus
Rb	Retinoblastoma
RIPA	Radioimmunoprecipitation assay
RNaseA	Ribonuclease A
Rpm	Revolutions per minute
RPMI	Roswell Park Memorial Institute
RT	Room temperature

S	Seconds
7-AAD	7-Aminoctinomycin
SD	Standard deviation
SDS	Sodium dodeyl sulfate
SRB	Sulforhodamine B
SubG1	Sub G1 phase
TBS	Tris base solution
TBS-T	Tris buffer saline with Tween-20
TCA	Trichloroacetic acid
TGS	Tris-glycine-SDS
V	Volt

Chapter 1:
INTRODUCTION

1.1 Epithelial Ovarian Cancer

Ovarian cancer (OC) is an important global health concern, representing a significant contributor to cancer-related death and ranking as the eighth most prevalent cancer diagnosed in women (Sung et al., 2021; Folsom et al., 2023). In 2020, 313,959 new cases were detected and 207,252 cases who were diagnosed with OC died due to the disease, contributing 3.4% of the total number of cases and 4.7% of the total deaths related to cancer (Sung et al., 2021). These high death rates end up OC as the third most prevalent gynecological cancer type, following cervical and endometrial cancers. Epithelial ovarian cancer (EOC), besides, is known as the most common type of ovarian cancer, corresponding to almost all ovarian malignancies with 90% prevalence percentage. (Huang et al., 2022). It is an aggressive malignancy with only a few effective treatment options and is considered incurable due to its heterogeneous nature on the molecular level and mostly its diagnosis at a very late stage, showing metastatic properties in the abdomen (Yeung et al., 2015). Its current therapy involves cytoreductive surgery followed by platinum-based chemotherapy (Jayson et al., 2014). While only 20% of the patients are diagnosed at the early stage, which is a non-metastatic stage still only restricted to ovaries, up to 90% of these patients are considered curable with currently available treatments. Advanced EOC with metastases, in contrast, shows a lower survival rate due to its aggressive behavior and late diagnosis (Bast et al., 2009).

Several classifications have been made based on the different histological and molecular characteristics of EOCs but the most commonly used system in the clinic classifies EOCs into four main histotypes: (1) serous (consisting both high-grade and low-grade carcinomas), (2) clear cell, (3) endometrioid, and (4) mucinous (Figure 1.1) (Committee on the State of the Science in Ovarian Cancer Research, 2016). These subtypes are categorized differently based on their origin, alterations, and potential for targeted therapeutics (Figure 1.1) (Figure 1.2). According to each subtype and their risk of recurrence, different systematic therapies are determined (Matulonis et al., 2016). Although treatment strategies applied might vary according to each subtype, the primary

treatment for epithelial ovarian cancer is the surgical removal of tumor as much as possible followed by platinum and taxane-based chemotherapy (Bast et al., 2009). Among the main histological subtypes of EOC, most patients (~ 70% of the patients) have high-grade serous carcinoma as the prevalent histological subtype.

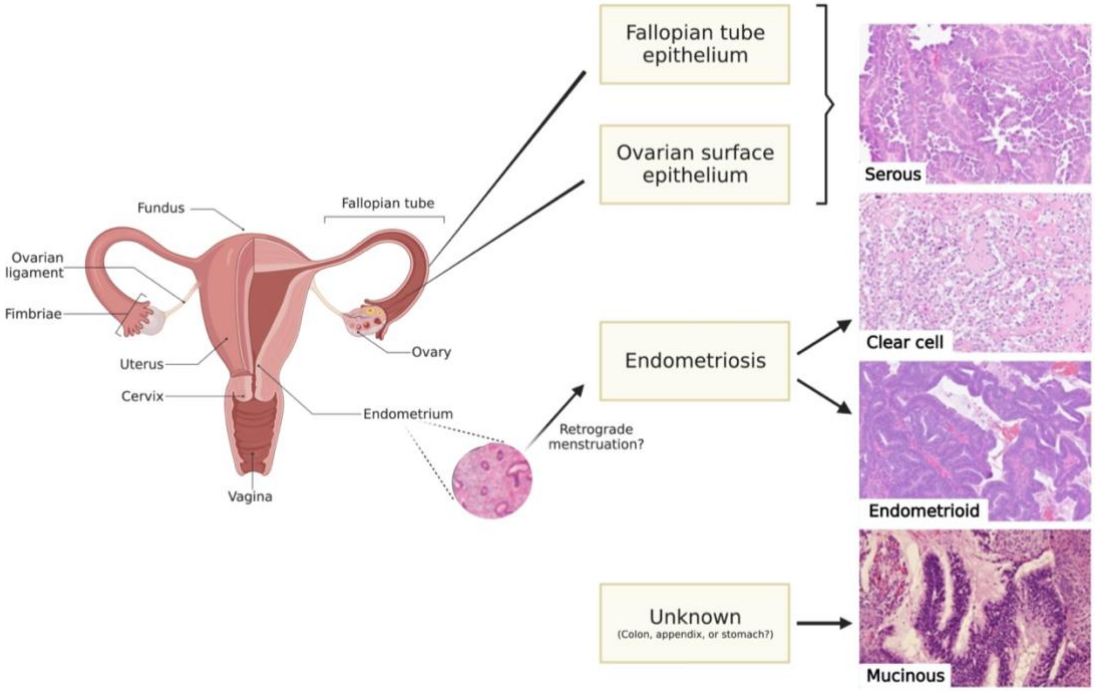

Figure 1.1: *The histological subtypes of epithelial ovarian cancer and their potential cellular origins (created with BioRender.com). Note.* Photographs of pathology slides reprinted from "[Ovary-Epithelial Carcinoma]", by BC Cancer, 2023, (http://www.bccancer.bc.ca/health-professionals/clinical-resources/cancer-management-manual/gynecology/ovary-epithelial-carcinoma). Copyright 2023 by BC Cancer.

1.1.1 High-Grade Serous Ovarian Cancer

High-grade serous ovarian carcinoma (HGSOC) emerges as the predominant subtype of EOC, characterized by its aggressive behavior and limited treatment options, resulting in poor patient outcomes (Bowtell et al., 2015; Kurman & Shih, 2016). HGSOC is believed to be derived from either the epithelium of fallopian tube or ovarian surface (Zhang et al., 2019). Despite the current standard treatments, a considerable proportion

of HGSOC patients inevitably develop chemoresistance, leading to a high mortality rate and an urgent need for improved treatment strategies, and therapeutic interventions. (Jayson et al., 2014; Vaughan et al., 2011).

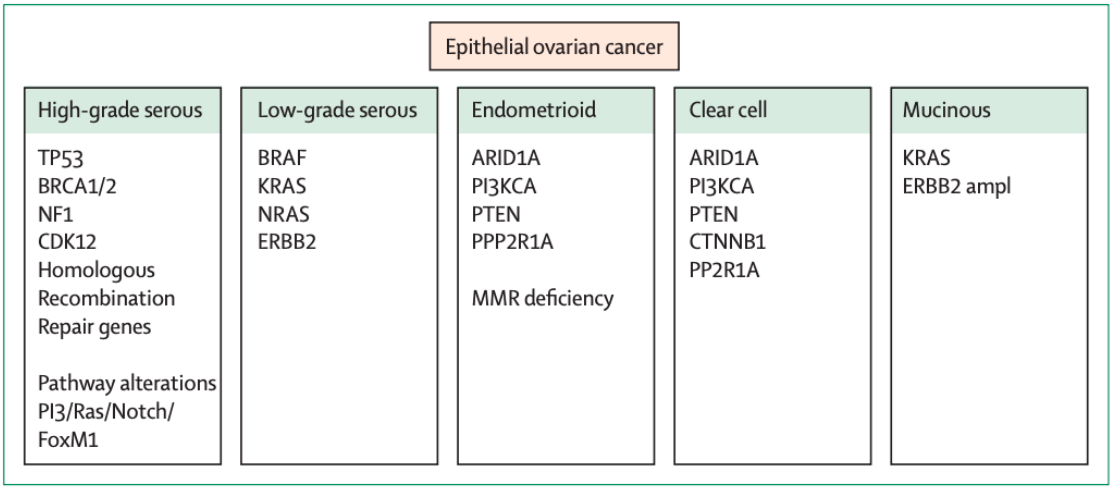

Figure 1.2: *Mutation characteristics of epithelial ovarian cancer*. *Note.* Reprinted from "Ovarian cancer", by Jayson, G. C., Kohn, E. C., Kitchener, H. C., & Ledermann, J. A., 2014, *Lancet*, *384*(9951), 1376–1388.

HGSOC is mostly characterized by abnormal p53 profiles, which is known as a tumor suppressor gene referred as "the guardian of the genome" (Figure 1.2) (Saleh & Perets, 2021). *TP53* gene is frequently mutated in HGSOC patients, with up to 96% of cases, and has a crucial part in tumorigenesis (Cancer Genome Atlas Research Network, 2011). Commonly, mutations in the *TP53* gene also activate mutations in different pathways such as the retinoblastoma (Rb) pathway, and cause their deregulation. The PI3K/Ras pathways, on the other hand, are the key altered pathways identified in HGSOC, including RAS/ERK and PI3K/AKT signaling (Nakamura et al., 2017). Additionally, approximately 25% of HGSOC patients harbor germline mutations in *BRCA* genes, leading to disrupted DNA repair mechanisms and increased susceptibility to ovarian cancer (Alsop et al., 2012; Pennington et al., 2014). Normally, the BRCA genes play an important role in double-stranded DNA damage repair through homologous recombination (Jayson et al., 2014). The mutations in these genes disrupt critical cellular

processes involved in cell proliferation, survival, and metastasis, such as cell cycle regulation and DNA repair, leading to genomic instability and tumor evolution.

Up to 75% of the patients with advanced-stage HGSOC show recurrence. While treatment, selection of the most appropriate treatment and apply this therapy at the most appropriate phase remains as a challenge (Luyckx, et al., 2022). Patients with advanced HGSOC with distance metastasis do not usually respond to standard therapy. Therefore, there is a desperate need for novel treatment options. Recently, in addition to the use of standard platinum and taxane-based chemotherapy drugs including carboplatin and paclitaxel, Poly (ADP-ribose) polymerase inhibitors, referred as PARP inhibitors, have been discovered as promising drugs in the treatment of ovarian cancer, particularly in tumors harboring defects in homologous recombination (HR) repair pathways, such as tumors with *BRCA1/2* mutations (Liu et al., 2014). PARP inhibitors exploit synthetic lethality, selectively targeting cancer cells with defective HR repair mechanisms and leading to their cytotoxicity (Lord & Ashworth, 2017; Pujade-Lauraine et al., 2017). Clinical trials have shown the efficacy of PARP inhibitors, including olaparib and niraparib in improving overall survival in HR-deficient HGSOC patients. However, the development of acquired resistance to PARP inhibitors also represents a significant challenge in the treatment of ovarian cancer, limiting their long-term effects (Mirza et al., 2016).

To solve the issue of chemoresistance and develop novel therapeutic strategies, it is important to investigate the molecular mechanisms taking part in resistance development. By unraveling the complex interplay between DNA repair dysregulation, genomic instability, and acquired resistance, new therapeutic targets can be identified and used to overcome resistance and improve patient outcomes in ovarian cancer. Therefore, by aiming to reverse the resistance, discovering new treatment strategies is of great importance to characterize new drugs which might be used in HGSOC therapy.

1.2 Small Molecule Inhibitors

Tumor resection surgery combined with chemotherapy, hormonal therapy, and/or radiotherapy has long been the main treatment strategy (conventional therapy) for cancer

(Debela et al., 2021). Chemotherapy, specifically, is the most commonly-used cancer treatment, which aims to kill cancer cells or to reduce their proliferation rate by chemical drugs. Although It is the most frequently applied treatment strategy, the search for more effective treatments has continued due to its ineffectiveness to distinguish between tumor cells and normal cells in the body, thus causing many different side effects and cytotoxicity (Zhong et al., 2021). Accordingly, with the discovery of different molecular drivers and oncoproteins for each cancer type in recent years, the development and characterization of small molecule inhibitors that specifically target the cancer-promoting mechanisms in which these proteins are involved have gained great importance (Sun et al., 2021).

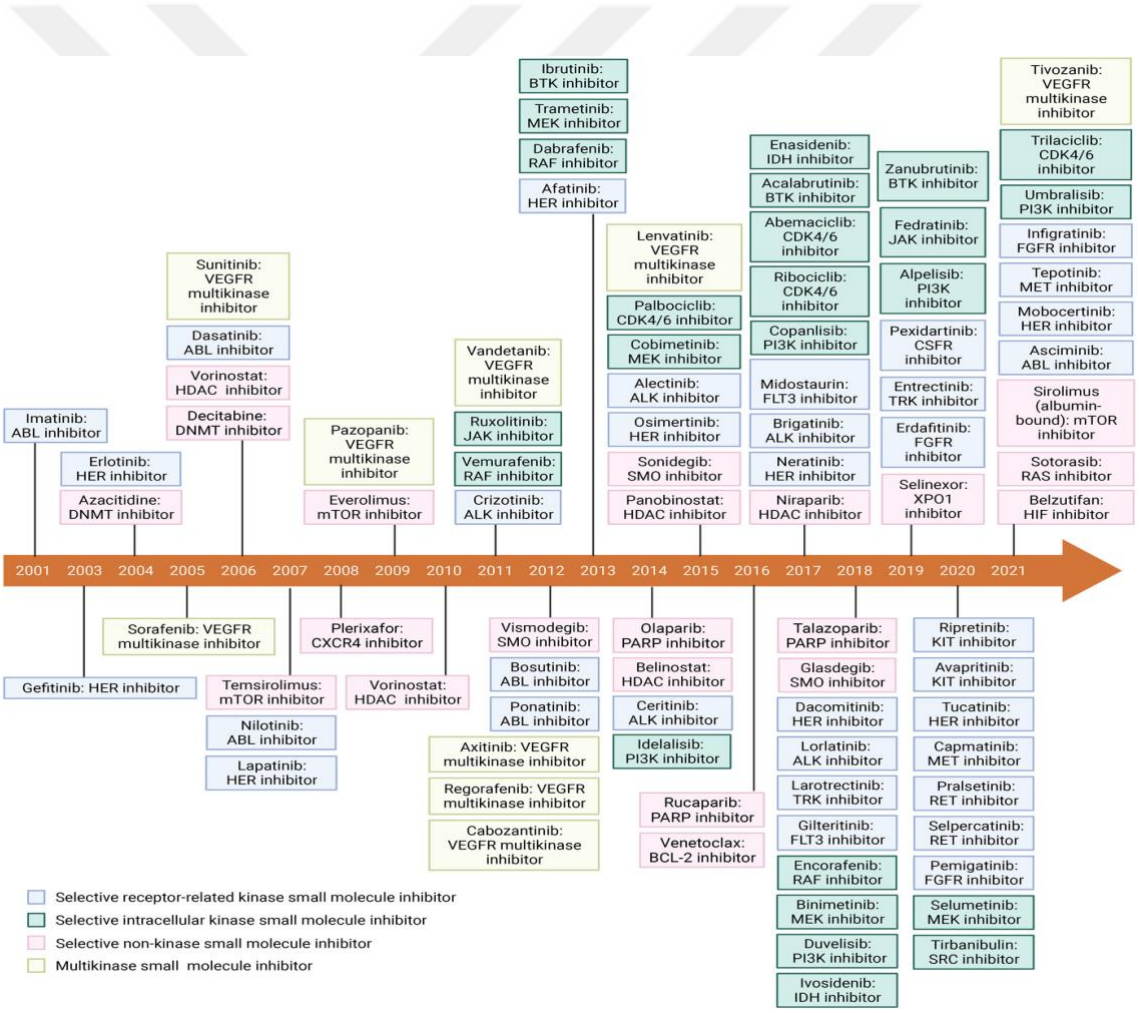

Figure 1.3: *Timeline for the discovery of small molecule inhibitors targeting cancer cells*. *Note.* Reprinted from "Small molecule inhibitors targeting the cancers", by Liu, G. H., Chen, T., Zhang, X., Ma, X. L., & Shi, H. S., 2022, *MedComm*, *3*(4), e181.

As part of "targeted cancer therapy", the discovery of novel small molecules that are more effective and less cytotoxic, targeting only cancer cells without harming normal cells, is increasing day by day (Figure 1.3) (Liu et al., 2022). Small molecule inhibitors target and stick to the pocket on the surface of target proteins, leading to their inhibitory effect on downstream protein-protein interactions in cell signaling pathways involved in cancer progression, including gene expression regulation, signal transduction, DNA repair, and cell growth (Wu et al., 2023). Therefore, the discovery of novel molecular targets of cancer and the subsequent development of novel targeted molecules for these targets are promising for new treatment strategies for patients with cancer.

1.3 Chalcones

Chalcones are precursors of flavonoids which are basic chemical structures found in many natural compounds, especially in plants such as fruits, vegetables, and tea (Rozmer & Perjési, 2014). They are types of ketones with two aromatic rings which are linked by a three-carbon α,β-unsaturated carbonyl system (Figure 1.4) (Rudrapal et al., 2021; Ouyang et al., 2021).

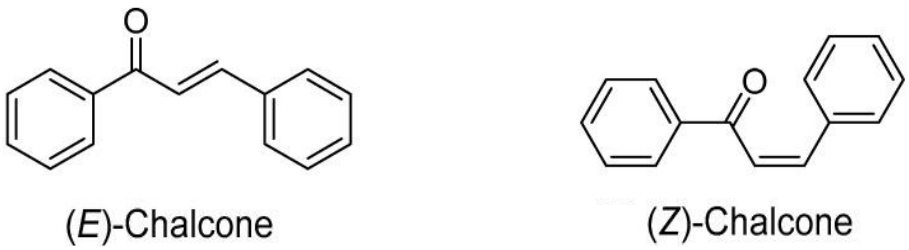

Figure 1.4: *The main structures of chalcones*. *(E)*-chalcone representing trans- isomers while *(Z)*-chalcone as cis- isomer. *Note.* Retrieved from "Chalcone derivatives: role in anticancer therapy", by Ouyang, Y., Li, J., Chen, X., Fu, X., Sun, S., & Wu, Q., 2021, *Biomolecules*, *11*(6), 894.

As a pioneer in the discovery of the therapeutic effects and medicinal uses of chalcones, in the early 1970s, It was reported that a chalcone has been isolated as a novel compound from *Pityrogramma triangularis*, following the isolation of isoliquiritigenin

and isoliquiritin, also types of chalcones, from *Glycyrrhiza glabra* which is an already proven medicinal plant used against various human disorders (Fenwick et al., 1990; Rudrapal et al., 2021).

The successful medical use of natural chalcones has paved the way for the development of novel synthetic chalcones with enhanced biological properties. Thus, currently, besides being naturally occurring, chalcones can be also synthetically synthesized (Karthikeyan et al., 2015). Recently, chalcones have received great attention due to the manipulation of their main structure easily, the ease of their synthesis, as well as their wide range of biological properties (Maciejewska et al., 2022). Although the biological activities they show are very diverse, the most prominent ones are anti-bacterial, anti-viral, anti-diabetic, anti-fungal, anti-inflammatory, antioxidant, and most importantly anticancer (Figure 1.5) (Jandial et al., 2014).

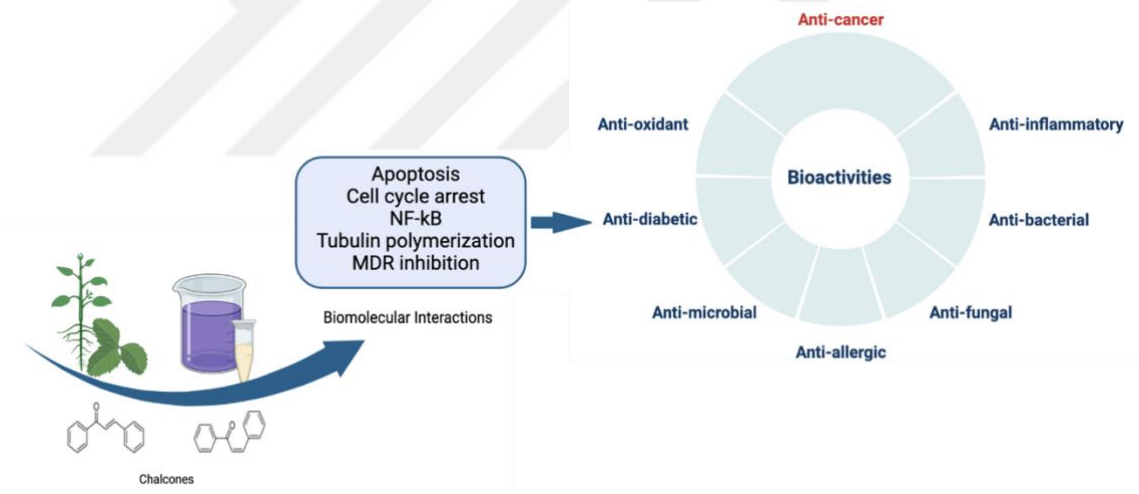

Figure 1.5: *Chalcones possess a wide range of biological activities through multiple biomolecular mechanisms*. (created with BioRender.com) (Jandial et al., 2014).

Chalcones can act on various drug targets and key molecular interactions that may normally play roles in important cellular processes such as multi-drug resistance (MDR) mechanism, angiogenesis, and apoptosis (Figure 1.5) (Jandial et al., 2014). In Figure 1.6, the chemical structures and activities of several chalcones which have been already approved and clinically used are shown.

Chemical structure	Activity	Mechanism of action
Metochalcone 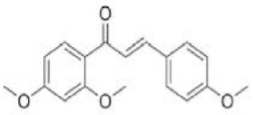	Choleretic Diuretic	PCSK9 inhibitor
Sofalcone 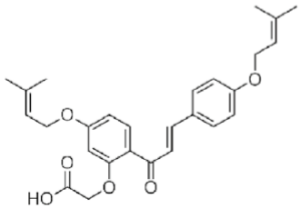	Anti-ulcer Mucoprotective	H2-receptor antagonist
Isoliquiritigenin 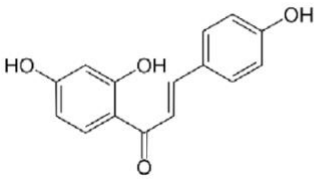	Antioxidant Anti-inflammatory	EC 1.14.18.1 inhibitor NMDA receptor antagonist GABA-A benzodiapine receptor positive allosteric modulator
Xanthohumol 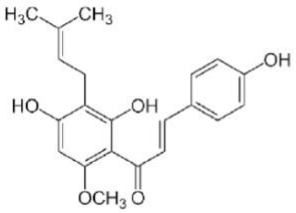	Anticancer Antioxidant Anti-inflammatory	Farnesoid X receptor agonist Inhibitor NFkB Inhibitor NRF2
Hesperidin methylchalcone 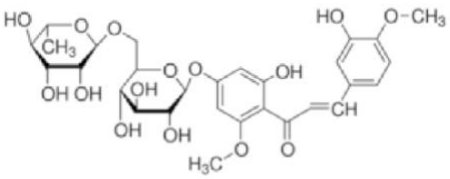	Vascular protective Antioxidant Anti-inflammatory Neuroprotective	Inhibitor oxidative stress Inhibitor cytokine production Inhibitor NF-κB

Figure 1.6: *Chemical structures of clinically used chalcones. Note.* Retrieved from "Novel chalcone-derived pyrazoles as potential therapeutic agents for the treatment of non-small cell lung cancer", by Maciejewska, N., Olszewski, M., Jurasz, J., Serocki, M., Dzierzynska, M., Cekala, K., Wieczerzak, E., & Baginski, M., 2022, *Scientific reports*, *12*(1), 3703.

1.3.1 Anticancer Activity of Chalcones

Chalcones demonstrate a broad range of biological and pharmacological activities and potential *in vitro* and *in vivo* activity against cancer through different cellular mechanisms including apoptosis induction, angiogenesis inhibition, cell cycle arrest, tubulin polymerization inhibition, and MDR inhibition (Figure 1.7) (Maciejewska et al., 2022).

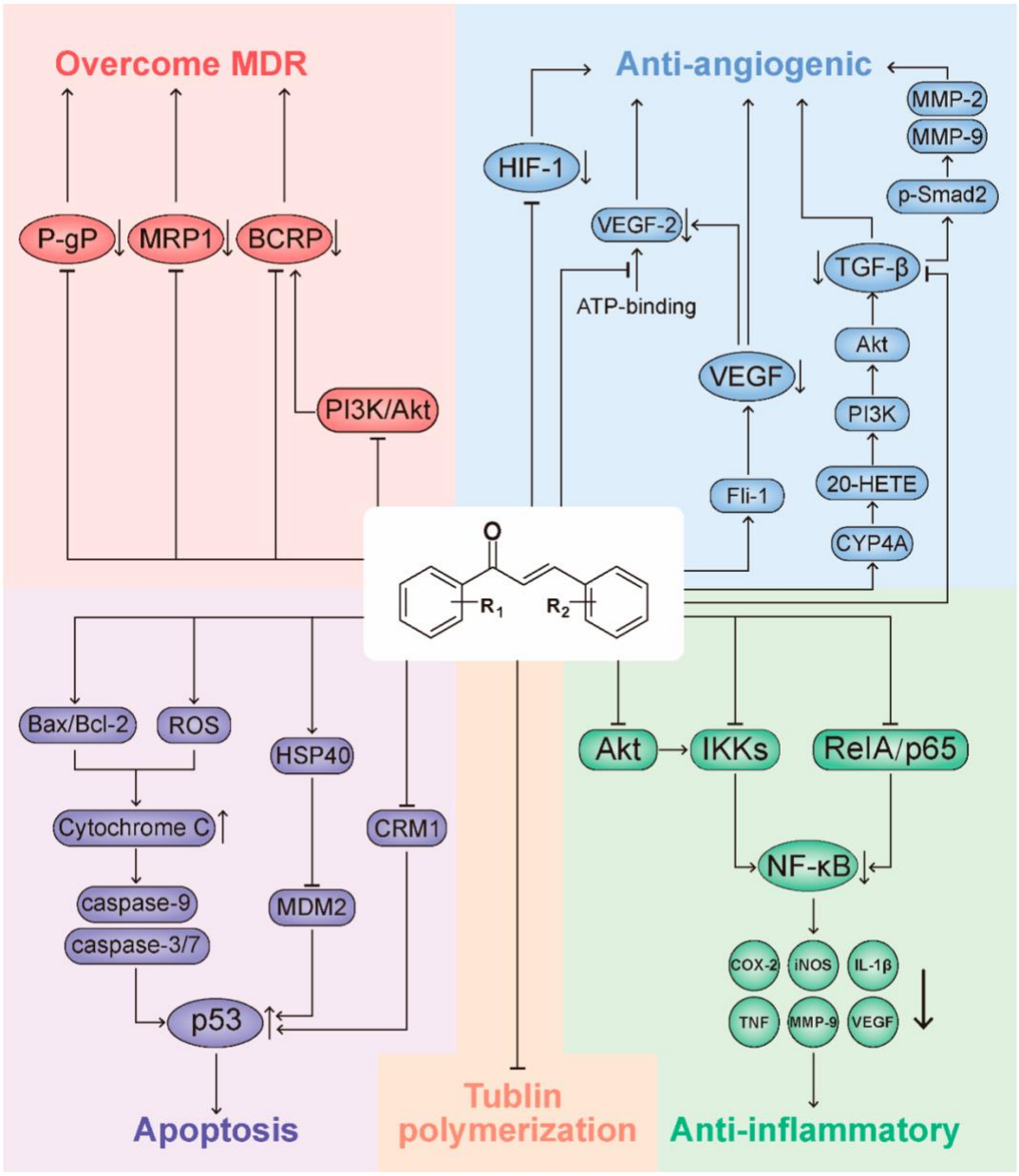

Figure 1.7: *The molecular targets of chalcones for their anti-cancer effects. Note.* Reprinted from "Chalcone derivatives: role in anticancer therapy", by Ouyang, Y., Li, J., Chen, X., Fu, X., Sun, S., & Wu, Q., 2021, *Biomolecules*, *11*(6), 894.

As an example of natural chalcones, Xanthohumol, which is found in the *Humulus lupulus* plant, is demonstrated as a wide-range cancer chemo-preventive agent (Figure 1.6) (Harish et al., 2021). Isoliquiritigenin (ISL), having a chalcone structure, was also shown to have anti-cancer properties against multiple cancers, including ovarian cancer, breast cancer, gastrointestinal cancer, and lung cancer by suppressing cancer cell proliferation, inducing apoptosis, reducing metastasis, and lastly enhancing the sensitivity of cancer cells to chemotherapy (Wang et al., 2021). In a recent study, It was revealed that *in vitro* ISL treatment reduced the cell growth in ovarian carcinoma through the induction of apoptosis, which resulted in the inhibition of ovarian cancer metastasis by inducing epithelial to mesenchymal transition (Chen et al., 2019; Wang et al., 2021). At the same time, Nardoaristolone A, a naturally occurring chalcone extracted from *Nardostachys chinensis,* has been shown to be an effective compound in the use of medical applications for various skin and endometrium cancers (Matos et al., 2015).

Since the natural chalcones demonstrate a variety of anticancer activities and the modification of their structure is easy, their core structure has been significantly modified to change and enhance the anticancer activities of these molecules (Abdollahi et al., 2012). Their biological activities and the molecular targets to which they bind change after the addition of various functional groups such as halogens, carboxyls, aryls, hydroxyls, etc., which gains chalcones more improved pharmacological or biological actions (Gomes et al., 2017). These minor modifications mentioned above or even more complex ones that are arisen from the hybridization of chalcones with already approved anticancer molecules (resulting in chalcone hybrids) have promising effects in overcoming drug resistance and improving therapeutic strategies in cancer (Gao et al., 2020). Thus, either natural or synthetic, chalcones are important compounds to develop novel synthetic chalcone derivatives with enhanced anticancer properties.

In the literature, anticancer effects of a wide range of synthetic chalcones have been reported. In a recent study, It was shown that a novel methoxyphenyl chalcone derivative reduced the cell growth of ovarian cancer cells by apoptosis induction when introduced either as monotherapy or in combination with cisplatin, resulting in a synergistic effect (Su et al., 2017). In the same study, It was also cited that chalcone compound had a modulatory effect on the G2/M phase of the cell cycle (Su et al., 2017).

In another study, through the induction of SubG1 arrest and the inhibition of Akt phosphorylation, novel synthetic chalcones led to cell death in hepatocellular carcinoma (HCC), a type of liver cancer (Sahin et al., 2020). These chalcones have caused both p21 activation and NFκB inhibition whose downstream pathways play important roles in the cell cycle arrest and apoptosis induction (Sahin et al., 2020; Abbas & Dutta, 2009; Naugler & Karin, 2008). Moreover, another novel chalcone derivative was shown to have a high cytotoxic activity against MCF-7 cell line, type of breast cancer cells, and a promising activity for its tubulin polymerization inhibition (Wang et al., 2020). In a different study, It was shown that two novel chalcone derivatives induced cell death in glioblastoma cell lines, which are a type of brain cancer cells, by either the induction of apoptosis through the activation of effector caspase, caspase-3, and the initiator caspases, caspase-8 and caspase 9 or through the increase in reactive oxygen species levels respectively (Champelovier et al., 2013). Besides, many scientists have demonstrated the effects of chalcones on the activation of the pro-apoptotic protein Bax, whose activation resulted in mitochondria-mediated apoptosis induction (Hsu et al., 2009; Yun et al., 2006). Moreover, a novel coumarin-chalcone hybrid was also reported to induce DNA damage and activate p53, which is an important tumor suppressor protein, through its phosphorylation (Singh et al., 2014; Ashraf et al., 2017; Muñoz-Fontela et al., 2016). In the same study, the anticancer activity of novel chalcone hybrids was also shown *in vivo* in tumor xenografts of NOD/SCID mice (Singh et al., 2014). Therefore, there are various studies demonstrating the anticancer and therapeutic effects of chalcones in several cancer types through different biological mechanisms.

1.4 Aim of The Study

In light of the anticancer activities of chalcones in the literature, the aim of this study was to initially investigate the anticancer effects of a library of novel chalcone derivatives on human ovarian cancer cells, where the biological activities of compounds that demonstrated promising therapeutic effects against ovarian cancer cells were further investigated.

Chapter 2:
MATERIALS AND METHODS

2.1 Materials

2.1.1 Equipment and Materials

Equipments and materials used in this thesis are demonstrated below.

Table 2.1: Equipment and materials used in this project.

Equipment	**Supplier Company**
Pipettes	Eppendorf Reference, Research
Pipette Tips	Sarstedt
Sterile Disposable Serological Pipettes	Sarstedt
Microfuge Tubes	Eppendorf Safe-Lock Microcentrifuge Tubes
TC-Treated Cell Culture Plates for Adherent Cells	Sarstedt
TC-Treated Cell Culture Dishes for Adherent Cells	Sarstedt
Cell strainers	Sarstedt
Forceps	Electron Microscopy Sciences (EMS)
Scalpel Handle	Electron Microscopy Sciences (EMS)
Analytical Balance	Shimadzu ATX224
Microscope Slides	Thermo Fischer
Confocal Microscope	Leica DMi8 /TCS SP8-DLS
Waterbath (Thermostat)	Memmert
Centrifuge	Themo Scientific
Inverted Microscope	Nicon Eclipse TS100
Biosafety Cabinet	LABCONCO Class II, Type A2 Biosafety Cabinets
CO_2 Incubator	New Brunswick Galaxy 170 S

Magnetic stirrer with heating	WiseStir MSH-20A
Vortex	Stuart SA8
Heating Block	Denville Scientific Inc. D1100
pH Meter	Mettler Toledo
Microplate Reader	Synergy H1 Plate Reader
Scanner	HP Scanjet G4050
Flow Cytometry	Beckman Coulter CytoFLEX Flow Cytometer
Cell Analyzer	Guava® Muse® Cell Analyzer
Transfer System	Trans-Blot® Turbo™ Transfer System
Electrophoresis System	Mini-PROTEAN Vertical Electrophoresis System
Imaging System	Licor Odyssey® Fc Imaging System

2.1.2 Commercial Kits

Kits used in this project are demonstrated in Table 2.2.

Table 2.2: Commercial kits used in this thesis.

Kits	**Supplier Company/Catalog Number**
Muse® Annexin V & Dead Cell Assay Kit	Millipore, #MCH100105
Muse® Caspase-3/7 Assay Kit	Millipore, #MCH100108
Pierce™ BCA Protein Assay Kit	Thermo Fischer, #23225

2.1.3 Chemicals and Media Components

Chemicals and media components used are shown in Table 2.3.

Table 2.3: Chemicals and media used in the study.

Chemical/Solution	Supplier Company/Catalog Number
FGF	Sigma, #F0291
EGF Human	Sigma, #SRP3027
Hydracortisone	Sigma, #H0888
Insulin from Bovine Pancreas	Sigma, #I1882
Dimethyl Sulfoxide (DMSO)	Sigma, #D8418
1X Dulbecco's Phosphate Buffer Saline (DPBS) w/o Calcium, w/o Magnesium	Biowest, #L0615
1X Hanks' Balanced Salts Solution (HBSS) w/o Calcium, w/o Magnesium	Biowest, L0605
RPMI 1640	Capricorn, #RPMI-A
Dulbecco's Mod. Of Eagle Medium/Ham's F12 50/50 Mix (DMEM:F12)	Multicell, #319-075-CL
Fetal Bovine Serum (FBS)	Biowest, S1600H
Penicillin-Streptomycin Solution 100X (P/S)	Biowest, #L0022
Amphotericin B	Gibco, #15290018
0.05% Trypsin-EDTA Solution	Multicell
Collagenase/Dispase, 100 mg	Roche, 10269638001
Sulforhodamine B Sodium Salt	Sigma, S1402
Trichlorocetic acid (TCA)	Sigma, T4885
Acetic Acid (Glacial)	Isolab, 901.013.2500
Tris	Biorad, 161-0719
Carboplatin (Clinical Grade)	Kocak Farma, 8680150010030

Cisplatin (Clinical Grade)	Kocsel Ilac, 8699715772092
Crystal Violet	Pro Lab Diagnostics
Methanol	Isolab, 947.046.2500
Ethanol	Isolab, 920.026.2500
Propidium iodide (PI)	Sigma, P4864
TritonX-100	Sigma, X100
RNAse A	Thermo Fischer, 1209021
Paraformaldehyde	Sigma, #158127
Tween-20	Sigma, #P1379
Superblock	ScyTek Laboratories
Mounting Medium with DAPI	Abcam, #ab104139
RIPA Lysis Buffer	Ecotech ClearBand, RIPA-100
PhosSTOP	Roche, #4906837001
Protease Inhibitor Cocktail	Roche, #05892791001
4x Laemmli Sample Buffer	Biorad, #1610747
2-Mercaptoethanol	Biorad, #1610710
4-15% Protein Gels	Mini-PROTEAN® TGX™ Precast Protein Gels
10x Tris/Glycine/SDS Buffer	Biorad, #161077EDU
Blotting-Grade Blocker (Nonfat Dry Milk)	Biorad, #1706404
Bovine Serum Albumin	Sigma, #A2153
Sodium Azide	Sigma, #71289
Ponceau S	Ecotech ClearBand, #PS05
Pierce™ ECL Western Blotting Substrate	Thermo Fisher, #32106

Sodium Chloride (NaCI)	Isolab, #969.036
Sodium Hydroxide (NaOH)	Isolab, #969.112
Sodium Phosphate Monobasic	Sigma, #S0751
Sodium Phosphate Dibasic	Sigma, #79510

2.1.4 Buffers and Solutions

Prepared buffers and solutions are given in Table 2.4 below.

Table 2.4: Buffer and solutions prepared in the study.

50%TCA Solution	
Trichloroacetic Acid ddH_2O	Diluted from 100% TCA solution to 50% TCA in ice-cold dH_2O.
1% Acetic Acid Solution	
Acetic Acid ddH_2O	1% (v/v) acetic acid in ddH_2O.
SRB Solution	
Sulforhodamine B Sodium Salt (SRB) Acetic Acid	0.4% (w/v) SRB stain in 1% Acetic acid solution.
10 mM Tris base solution (pH:10.5)	
Tris Base ddH_2O	0.3 g Tris base in 500 mL ddH_2O.
Propidium Iodide (PI) Solution	
Propidium Iodide, Triton100-X, RNaseA ,1x DPBS	Dissolved 50 μg PI/ml, 0.1 mg/ml RNase A, and0.05% Triton100-X in ice-cold 1x DPBS.

1 N NaOH Preparation	
Sodium Hydroxide (NaOH) ddH_2O	1 ml NaOH + 9 ml ddH_2O
0.2 M Phosphate Buffer (pH:7.4)	
Sodium Phosphate Monobasic Sodium Phosphate Dibasic ddH_2O	Dissolved 4.15 g sodium phosphate monobasic and 22.5 g sodium phosphate dibasic in 1 L ddH_2O.
4% Paraformaldehyde Solution (pH:7.4)	
Paraformaldehyde 0.2 M Phosphate Buffer 1 N NaOH ddH_2O	Dissolved 40 g paraformaldehyde in 400 ml ddH_2O. Solution heated till 58-60°C and 1 N NaOH was added until a clear appearance obtained. Added 500 ml 0.2 M phosphate buffer into the solution.
Permeabilization Solution (IF)	
TritonX-100 ddH_2O	0.1% TritonX-100 in 100 ml ddH_2O
Wash Solution (IF)	
Tween-20 ddH_2O	0.1% Tween-20 in 100 ml ddH_2O
RIPA Lysis Solution	
RIPA Buffer Protease Inhibitor Cocktail (100X) PhosSTOP (20X)	1X Protease Inhibitor Cocktail and 1X PhosSTOP in 100 ul RIPA Buffer
1x Running Buffer	
10x Tris/Glycine/SDS (TGS) ddH_2O	100 ml 10x TGS + 900 ml ddH_2O

10x TBS (pH:7.6-7.8)	
Tris Base NaCI ddH_2O	24 g Tris base + 88 g NaCI + 1 L ddH_2O
1x TBS-T	
10x TBS Tween-20 ddH_2O	1 ml Tween-20 + 100 ml 10x TBS + 900 ml ddH_2O
Transfer Buffer	
10x TBS Methanol ddH_2O	100 ml 10x TGS + 200 ml Methanol + 700 ml ddH_2O
Blocking Buffer	
Blotting Grade Blocker 1x TBS-T	5 g Blotting Grade Blocker + 100 ml 1x TBS-T
10% Sodium Azide Solution	
Sodium Azide (NaN_3) ddH_2O	5 g NaN_3 +50 ml ddH_2O
Primary Antibody Solution for Western Blot	
Bovine Serum Albumin (BSA) Sodium Azide (NaN_3) TBS-T	3% BSA + 0.02% NaN_3 in TBS-T

2.1.5 Antibodies

Antibodies used for western blot and immunofluorescence protocols in this study are listed in Table 2.5 below.

Table 2.5: Antibodies used in immunofluorescence and western blot in the study.

Primary Antibodies	Company/Catalog Number	Dilution
Procaspase 3 Mouse mAb	Santa Cruz, #sc7272	1:1000
Cleaved Caspase-3 Rabbit mAb (D175) (5A1E)	Cell Signaling, #9664S	1:50
Akt Rabbit Ab	Cell Signaling, #9272S	1:1000
P-Akt (S473) Rabbit Ab	Cell Signaling, #9271L	1:500
PARP (46D11) Rabbit mAb	Cell Signaling, #9532S	1:1000
p53 (DO-7) Mouse mAb	Cell Signaling, #48818S	1:1000
P-p53 (S15) (16G8) Mouse mAb	Cell Signaling, #9286P	1:500
H2A.X Rabbit Ab	Cell Signaling, #2595	1:1000
Phospho-Histone-H2A.X (Ser139) (D7T2V) Mouse mAb	Cell Signaling, #80312S	1:500
Bax Rabbit Ab	Cell Signaling, #2772S	1:1000
Cyclin D1	Cell Signaling	1:1000
E-cadherin Mouse mAb	Cell Signaling, #14472S	1:1000
Vinculin Mouse Ab	Abcam	1:1000

GAPDH Mouse Ab	Abcam, #ab8245	1:1000
Secondary Antibodies	**Company/Catalog Number**	**Dilution**
Goat Anti-Mouse IgG H&L (HRP)	Abcam, #ab9723	1:2500
Goat Anti-Rabbit IgG H&L (HRP)	Abcam, #ab6721	1:2500
Goat anti-Mouse IgG (H+L) Cross-Adsorbed ReadyProbes™ antibody conjugated to Alexa Fluor™ 594	Invitrogen, #R37121	1:10

2.2 Methods

2.2.1 Cell Culture

Human ovarian cancer cell lines OVCAR-3, OVSAHO, and KURAMOCHI were kind gifts from Professor Ingrid Hedenfalk (Lund University, Sweden) while human normal breast cell line MCF-12A was a kind gift from Rengul Çetin Atalay and Deniz Cansen Yıldırım (ODTU CanSyL, Turkey). All ovarian cancer cell lines were cultured in RPMI-1640 (Capricorn, #RPMI-A) supplemented with 10% heat-inactivated fetal bovine serum (Biowest, #S160H) and 1% Penicillin/Streptomycin (Biowest, #L0022). MCF-12A cell line was cultured in DMEM:F12 (Multicell, #319-075-CL) supplemented with 10% heat-inactivated fetal bovine serum, 1% Penicillin/Streptomycin, 10ng/ml EGF (Sigma, #SRP3027), 500ng/ml Hydrocortisone (Sigma, #H0888), and 10µg/ml insulin (Sigma, #I1882). The cells were grown and maintained in a 37°C humidified incubator with 5% CO_2 and routinely screened for *Mycoplasma* contamination.

2.2.2 Isolation of Ovarian Cancer Cells from Human Solid Tumor Specimens

Solid tumor samples of high-grade serous ovarian cancer were collected during surgeries at Koc University Hospital from areas macroscopically identified as ovarian cancer by pathologists (Tumors were collected by Prof. Dr. Çağatay Taşkıran, Dr. Doğan

Vatansever, and Dr. Burak Giray). Tumor samples were placed in a sterile container filled with ice-cold 1x DPBS or 1x Hanks' Balanced Salts Solution (HBSS). Working in a sterile biosafety hood, the samples were taken into a glass petri dish (100 mm x 100 mm) containing 15 ml of fresh 1x DPBS and using sterile forceps and scalpels, cut into small tumor pieces (2 mm x 2 mm or less). The minced tissue was taken into a 15 ml tube containing 5 ml Collagenase/Dispase (Roche, #10269638001) (3 mg/ml; 2.4U/ml dispase, 0.3 U/ml collagenase) in 1x DPBS and agitated at 37° C for 1 hour. As a next step, the cell sample was taken onto a cell strainer placed on a 50 ml falcon tube. Approximately 15 ml of 1x DPBS was added onto the mesh to dilute enzyme solution. The cell suspension was collected in the 50 ml sterile falcon tube. The sample was then centrifuged at 400 g for 5 minutes. The supernatant was discarded and the cell pellet was resuspended in 10 ml DMEM:F12 supplemented with 20% FBS, % 1P/S, and 0.1% Amp B. The cell suspension was cultured into a 100 mm x 100 mm petri dish in a 37° C incubator with %5 CO_2. The spent medium was changed after five days at the earliest from the initial plating. The medium continued to be changed for the following two weeks when necessary and the isolated cells were used for downstream experiments.

2.2.3 Sulforhodamine B (SRB) Cytotoxicity Assay

Sulforhodamine B (SRB) colorimetric assay was used throughout this study in order to investigate the anti-proliferative and cytotoxic effects of novel chalcone compounds on three human ovarian cancer cell lines: OVCAR-3, OVSAHO, and KURAMOCHI, and a non-cancerous human breast cell line: MCF-12A and to determine their effective concentrations Besides, cytotoxic effects of the compounds were also investigated against primary cells isolated from solid tumors obtained from a HGSOC patient and carboplatin/olaparib-resistant OVCAR-3 and OVSAHO cell lines established in our lab. Carboplatin and cisplatin were used as reference drugs. Briefly, all cell lines were seeded into 96-well plates at 5000 cells/well in 100 µl of their corresponding growth medium and distributed evenly. After 24 hours of incubation, the cells were treated with increasing five concentrations of compounds (0-40 µM) by ½ serial dilution. To do that, the medium was discarded and 150 µl of fresh growth medium containing corresponding compounds or agents (at the concentrations of 40, 20, 10, 5, 2.5 µM) was applied to the wells. Following drug treatment, the plates were incubated in a 5% CO_2 incubator for 48

hours or 72 hours (Initial screenings were performed for 72 hours). After respective incubation times, 37.5 µl of %50 TCA solution (Final percentage was 10%) was added to each well and incubated at +4 °C, dark for 1 hour in order to fix the cells. To remove TCA solution, the cells were washed 4 times with ddH_2O and left to dry at room temperature. The fixed cells were stained with 50 µl of SRB solution and incubated at RT, dark for 30 minutes. The excess dye was removed by washing the plates 5 times with 1% acetic acid and left to air-dry at RT. Finally, stained cells were dissolved in 150 µl of 10mM Tris Base solution, and absorbance reading was performed at 564 nm by using the Synergy H1 Plate Reader (Biotek, USA). The results were obtained by n=3 independent experiments. Since all the compounds were dissolved in DMSO, DMSO was applied as a negative control and the absorbance values of compounds were normalized to DMSO-treated samples. The cell viability was calculated as percentages and % values were fitted to a non-linear dose-response inhibition curve to generate IC_{50} values of the compounds. The equation used in order to calculate the IC_{50} values is given as

$$IC_{50} = \exp\left(\frac{50 - y_{int}}{slope}\right) \tag{2.1}$$

2.2.4 Clonogenic Assay

The colony-formation ability of OVCAR-3, OVSAHO, and KURAMOCHI cell lines as a response to increasing doses of compound treatment was investigated by using a clonogenic assay. Cells were seeded into 12-well plates with 1000 cells/well in 2 ml growth medium and distributed evenly. Afterwards, the cells were treated with respective concentrations of compounds of interest (at the concentrations of 1, 2.5, 5, 10, and 20 µM) for 24 hours or 48 hours. 1 ml fresh medium containing compounds was added onto the spent medium, resulting in corresponding compound concentrations. At the end of the treatment period, the medium was discarded and replaced with fresh medium. Until the cells showed colony formation, the medium was changed with fresh medium when necessary, and they were expected to form colonies. After the cells showed colony formation (approximately 15-16 days), the incubation time was stopped and the cells were washed twice with 1x DPBS. Afterwards, cells were fixed with 100% ice-cold methanol for 5 minutes. Cells were washed twice with 1x DPBS again and then stained with 0.5%

Crystal Violet solution for 15 minutes. To remove excess dye, the cells were washed with ddH_2O and left to dry at RT. The colonies were scanned to the computer, photographed, and counted by ImageJ software. The number of colonies depending on the compound treatments was analyzed. The compound-treated samples were normalized to negative controls (DMSO-treated samples).

2.2.5 Analysis of Cell Cycle Distribution by Flow Cytometry

Ovarian cancer cell lines OVCAR-3, OVSAHO, and KURAMOCHI were cultured into 6-well plates with 100000 cells per well. 24 hours after seeding, medium was aspirated and cells were treated with corresponding compound concentrations (IC_{75}) or DMSO control for 48 and 72 hours. After the respective incubation times, spent medium was taken in a 15 ml falcon tube. The cells were rinsed once with 1x DPBS and then collected in the same falcon tube after trypsinization. Cell suspension was centrifuged at 2000 rpm for 6 minutes. As a next step, supernatant was discarded and cell pellet was resuspended in 5 ml 1x DPBS. Samples were again centrifuged at 2000 rpm for 6 minutes. Supernatant was aspirated and the cell pellet was dissolved in 1 ml 1x DPBS. While vortexing the tubes containing cell suspension at medium speed, 2.5 ml of ice-cold absolute ethanol (70% final percentage) was slowly added to the tubes to fix the cells. After fixation, samples were stored at +4 °C for at least 24 hours. To begin with staining procedure, the fixed samples were then centrifuged at 1500 rpm for 5 minutes. Afterwards, the cell pellet was resuspended in 500 µl of Propidium Iodide (PI) solution and incubated at 37°C, dark for 40 minutes. 3 ml 1x DPBS was added to each well and the samples were then centrifuged at 1500 rpm for 5 minutes. Lastly, the cell pellet was resuspended in 500 µl of 1x DPBS and the samples were transferred to the Beckman Coulter CytoFLEX Flow Cytometer (Beckman Coulter, USA) for running 10000 events per sample. Data was analyzed using CytExpert program and gates were determined according to DMSO control in order to evaluate the effects of compounds on cell cycle through DNA analysis. The results were obtained by n=3 independent experiments.

2.2.6 Apoptosis Assays

Two different apoptosis-related assays were used throughout this, Muse Annexin V & Cell Death Assay for detecting cells in different stages of apoptosis and Muse Caspase-3/7 Assay for determining apoptosis stages based on Caspase-3/7 activation.

2.2.6.1 Muse Annexin V & Dead Cell Assay

Annexin V assay was performed by using Muse® Annexin V & Dead Cell Assay Kit (Millipore, #MCH100105). Firstly, OVCAR-3 and OVSAHO cells were seeded into 6-well plates with 100000 cells/well in 3 ml growth medium. After 24 hours, the cells were treated with corresponding compound concentrations (IC_{75}) for 48 hours. Cells were collected by trypsinization and cell suspension was then centrifuged at 400 g for 4 minutes. The supernatant was removed, and the pellet was resuspended in 100 µl of ice-cold 1x DPBS. Cell concentration was adjusted to 300-500 cells/µl per sample. 100 ul of cell suspension was mixed with 100 µl of Annexin V & Dead Cell Reagent. After gently pipetting up and down the sample, samples were incubated at RT for 20 minutes and analyzed with Guava® Muse® Cell Analyzer (Luminex, USA) with 5000 events per sample. Gates were chosen according to DMSO control. The results obtained by n=3 independent experiments.

2.2.6.2 Muse Caspase-3/7 Assay

Caspase-3/7 assay was performed by using Muse® Caspase-3/7 Assay Kit (Millipore, #MCH100108) according to the manufacturer's instructions. OVCAR-3 and OVSAHO cells were seeded into 6-well plates with 100000 cells/well and allowed to attach for 24 hours. Next, the cells were treated with compounds of interest at IC_{75} concentration for 48 hours. After incubation, the cells were collected by enzyme, trypsin, rinsed once with 1x DPBS and centrifuged at 400 g for 4 minutes. Caspase-3/7 Reagent working solution was prepared by 1:8 stock solution dilution in 1x DPBS. At the same time, Caspase 7-AAD working solution was also prepared by 2:150 dilution by diluting Caspase 7-AAD stock solution in 1X Assay Buffer BA per sample. Cell concentration was adjusted to 300-500 cells/µl per sample. 50 µl of cell suspension was added into each tube and 5 ul of Muse® Caspase-3/7 Reagent working solution was added to the cells.

Samples were then incubated for 30 minutes in a 37°C incubator with 5% CO2. After incubation, 150 µl of Caspase 7-AAD working solution was added to each tube. Samples were mixed by pipetting up and down and incubated at RT for 5 minutes, protected from light. Lastly, samples were transferred to Guava® Muse® Cell Analyzer (Luminex, USA) for analysis of 5000 events per sample. Gates were decided according to DMSO control. The results were obtained by n=3 independent experiments.

2.2.7 Immunofluorescence

Ovarian cancer cell line, OVCAR-3, was cultured in 24-well plates on coverslips (preferably 12 mm-13 mm coverslips) at 100000 cells/well. 24 hours later, growth medium was changed with fresh medium containing the desired compounds or DMSO control at IC_{75} concentration for 48 hours. After the desired incubation time, cells were fixed with 4% Paraformaldehyde. Briefly, the spent media was discarded and the cells were rinsed twice with 1x DPBS. Then, the cells were fixed with 4% Paraformaldehyde at RT for 20 minutes by adding directly into the wells. The plates were rinsed three times with 1x DPBS and kept overnight at +4ºC until the immunostaining protocol the other day. The next day, the cells were rinsed twice with 1x DPBS and permeabilized for 15 minutes at RT, dark with 0.1% TritonX-100 in 1X DPBS. The cells were then washed once with 0.1% Tween-20 in 1x DPBS, and blocked with SuperBlock (ScyTek Laboratories) for 20 minutes at RT. After 20 minutes of incubation, the blocking solution was discarded and coverslips were placed on 17.5 µl of the following primary antibody solution, Phospho- Histone H2A.X (Ser139) Mouse mAb antibody (Cell Signaling, #80312S) diluted in SuperBlock (1:100) and incubated overnight at +4ºC. The next day, the slides were taken out of +4ºC and immersed into washing buffer a couple of times for washing. After that, coverslips were placed on 15 µl of the following secondary antibody solution (1:10), Goat anti-Mouse IgG (H+L) Cross-Adsorbed ReadyProbes™ antibody conjugated to Alexa Fluor™ 594 (Invitrogen, #R37121) diluted in 1x DPBS and incubated at 37ºC for 1.5 hours, RT. After desired incubation time, 6 ul of Mounting Medium with DAPI (Abcam, #ab104139) was placed on Thermo SuperFrost microscope slides (Thermo Fischer). The coverslips incubated with secondary antibody were immersed into a washing buffer to remove excess antibody solution and then placed on mounting medium by sealing with nail polish to stabilize the coverslips. They were kept

at +4ºC (dark) until visualization and visualized by confocal microscope (Leica DMi8 /TCS SP8-DLS). The results were obtained by n=3 independent experiments.

2.2.8 Western Blot

To analyze changes in protein levels, OVCAR-3 cell line was seeded in 150-mm petri dishes at 1500000 cells/well and incubated for 24 hours for attachment. Cells were then treated with the respective drug concentrations for 48 hours. At the end, cells were collected by enzyme trypsin (spent media included), washed once with 1x DPBS, and dissolved in 100 µl RIPA mixture on ice. By vortexing every 5 minutes, cell suspension was incubated on ice. The cells were then centrifuged at 14000 g at +4ºC. The supernatant was collected for further analysis. Protein concentrations were determined by Pierce's BCA Protein Assay Kit (Thermo Fischer, #2325.). 20 µg protein for each sample was mixed with 4x Laemmli Sample Buffer (containing 1:10 β-Mercaptoethanol), and ddH_2O, resulting in 2 µg protein/µl. Samples were then incubated at 95 ºC for 5 minutes. Samples were loaded as 10 µl for each well (20 µg/well) on a 4-15% Mini-PROTEAN® TGX™ Precast Protein Gels (Biorad, #4561086) and run at 80 V. After the proteins are separated using SDS-polyacrylamide gel electrophoresis and transferred onto a PVDF membrane via Bio-Rad Trans-Blot® Turbo™ Transfer System (Biorad, USA) for 30 minutes, The membrane was blocked with blocking solution (5% non-fat dry milk dissolved in 1x TBS-T) for 1 hour at room temperature. Then, the membrane was rinsed three times for 5 minutes each with 1x TBS-T. After that, the primary antibodies diluted at specified dilutions were added onto the membrane, shaken and incubated at 4^0C overnight. The next day, after washing three times with 1x TBS-T, the membrane was incubated in HRP-conjugated secondary antibodies diluted to 1:2500 in blocking solution. The membrane was again washed three times for 5 minutes each with 1x TBS-T and Pierce™ ECL Western Blotting Substrate (Thermo Fisher, #32106) was applied to the membrane for chemiluminescence signal detection and images were captured through Licor Odyssey® Fc Imaging System.

2.2.9 Investigation of Synergistic Effects of Chalcones and Carboplatin against Carboplatin-Resistant Ovarian Cancer Cells

To investigate if chalcones act synergistically with carboplatin against carboplatin-resistant OVCAR-3 cell line, mono and combinational treatments of a chalcone (MC013) and carboplatin were applied through SRB assay. Carboplatin-resistant OVCAR-3 cells were either treated with increasing concentrations of MC013 (0 µM, 2.5 µM, 5µM, and 10µM), carboplatin (0 µM, 5µM, 10µM, 20µM, and 40 µM) or both for 72 h. Absorbance values were normalized to negative controls and the inhibition was calculated as percentages. The combinational index (CI) values were obtained and CI values = 1, >1, and <1 demonstrated additive, antagonistic or synergistic interactions respectively.

Chapter 3:
RESULTS

3.1 Initial in vitro cytotoxicity screening of novel chalcone derivatives

To investigate the anti-proliferative activities of 16 novel chalcone compounds on human ovarian cancer cells, the cytotoxic effects of each compound were first evaluated by using SRB assay. Their biological activities were evaluated against three human HGSOC cell lines: OVCAR-3, OVSAHO, KURAMOCHI, and a non-tumorigenic normal breast cell line: MCF-12A. Carboplatin and cisplatin, which are commonly used chemotherapeutic drugs in ovarian cancer treatment, were used as references. Cells were treated with increasing five concentrations of compounds (0-40 µM) for 72 h respectively. The obtained results are presented as IC_{50} concentrations (half-maximal inhibitory concentration) (Table 3.1).

Table 3.1: *In vitro* cytotoxicity evaluation of novel chalcones and reference drugs for 72h, presenting as $IC_{50} \pm SD$ (µM) concentrations (NCI-SRB assay).

	OVSAHO	**OVCAR-3**	**KURAMOCHI**	**MCF-12A**
MC013	12.7 ± 1.1	7.4 ± 1.5	11.2 ± 1.8	22.6 ± 1.5
MC016	28.3 ± 17	13.4 ± 2	10 ± 1.2	20.5 ± 1.3
MC017	NI	NI	39.2 ± 28.8	NI
MC019	NI	33.5 ± 4.1	NI	>40
MC022	NI	NI	15.7 ± 0.2	NI
MC023	27.3 ± 3.8	13.8 ± 1.5	NI	21.3 ± 5.4
MC025	NI	NI	NI	NI
MC030	24.5 ± 1.9	10.4 ± 1.6	12.7 ± 3.8	28.8 ± 1.6
MC033	NI	NI	NI	NI
MC035	24.3 ± 1.8	19.6 ± 2.8	11.3 ± 1.4	5.2 ± 1.9
MC049	NI	NI	NI	34.6 ± 5
MC058	NI	NI	26.3 ± 1.4	9.2 ± 2.4
MC059	NI	NI	24.2 ± 2.8	21.4 ± 0.6
MC060	12.8 ± 1.2	8.9 ± 1.0	11.4 ± 3.5	27.5 ± 0.9
MC061	27.6 ± 3.2	17.2 ± 1	NI	21.2 ± 3.9
MC062	38.4 ± 2.8	14.4 ± 1.3	13.8 ± 0.6	36.1 ± 5.7
Carboplatin	50.6 ± 2.5	25.7 ± 0.8	36.1 ± 4.7	NI
Cisplatin	5.1 ± 0.9	4.6 ± 0.1	8.2 ± 0.01	N/A

*NI: No Inhibition, **N/A: Not available

3.2 MC013, MC030, and MC060 decreases the cell viability and proliferation of high-grade serous ovarian cancer cells

During the preliminary evaluation, it was revealed that among all the derivatives tested, MC013, MC030, and MC060 exhibited significant cytotoxic activity against ovarian cancer cells, with low IC_{50} values (Table 3.1). Other derivatives were either less effective or had no activity against cancer cells. Besides, MC013, MC030, and MC060 were less cytotoxic against non-tumorigenic human normal breast cells than they were to ovarian cancer cells, showing that these compounds had potent anti-proliferative

activities on ovarian cancer cells while they did not significantly affect the cell viability of human normal breast epithelial cells (Table 3.1) (Figure 3.1). Furthermore, all three derivatives were more effective against ovarian cancer cells respectively compared to the reference drug, cisplatin. Dose-response survival curves of corresponding compounds can be observed in Figure 3.1 below.

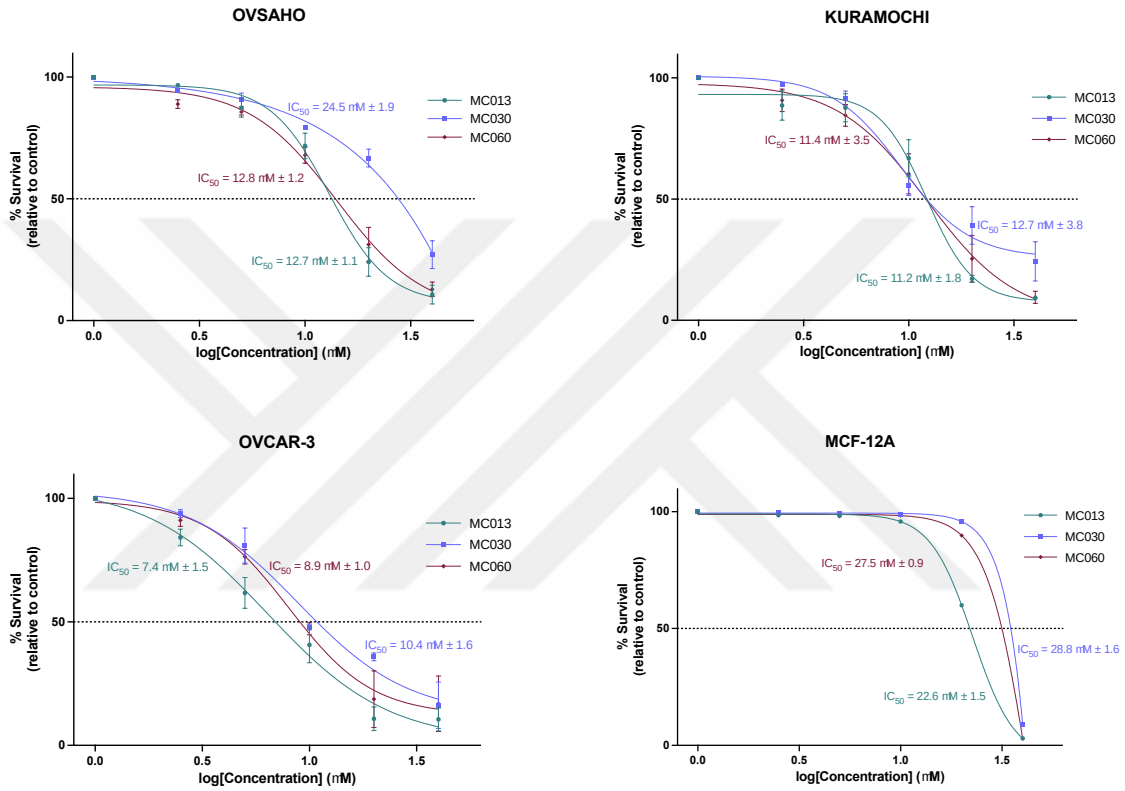

Figure 3.1: Dose response curves obtained by investigating the cell viability effects of MC013, MC030, and MC060 after 72 hours treatment by NCI-SRB assay. Cells were treated with five different concentrations (2.5 µM, 5 µM, 10 µM, 20 µM, and 40 µM) of MC013, MC030, and MC060 respectively and analyzed with SRB assay. The obtained cell index data were normalized to DMSO control and dose-response curves were plotted for OVSAHO, OVCAR-3, KURAMOCHI, and MCF-12A cells. Bars represent the SEM obtained in n = 3 independent experiments.

The cytotoxic activity of MC013, MC030, and MC060 was also investigated in OVSAHO and OVCAR-3 cells at 48h time point and their IC_{50} values were calculated (Table 3.2).

Table 3.2: *In vitro* cytotoxicity evaluation of MC013, MC030, and MC060 against OVSAHO and OVCAR-3 cells at 48h time point, presenting as $IC_{50} \pm$ SD (μM) concentrations (NCI-SRB assay).

	OVSAHO	**OVCAR-3**
MC013	17.4 ± 1	11.0 ± 0.3
MC030	28.8 ± 6.2	19.1 ± 1.2
MC060	20.8 ± 2.3	10.4 ± 0.4

As a further investigation, anti-proliferative activities of the promising chalcone derivatives, MC013, MC030, and MC060, were further tested against primary cells isolated from solid tumors of patient #1 diagnosed with HGSOC, and carboplatin/olaparib-resistant OVCAR-3 and OVSAHO cell lines established in our lab. It was found out that MC013, MC030, and MC060 also demonstrated significant cytotoxic and growth-inhibitory effects against primary HGSOC cells and *in vitro* models of chemoresistant ovarian cancer cells (Table 3.3). Cells from resistant cell lines showed a response similar to HGSOC cell lines, only giving slightly higher IC_{50} values (Table 3.3). It was also revealed that these three chalcone molecules might act on carboplatin/olaparib-resistant ovarian cancer cells through a different mechanism than carboplatin and olaparib itself since they demonstrated significant cytotoxic activities while cells were resistant to conventional chemotherapeutic drugs, carboplatin, and olaparib.

Table 3.3: *In vitro* cytotoxicity evaluation of MC013, MC030, and MC060 against primary cultures & *in vitro* chemoresistant models of ovarian cancer cells, presenting as IC_{50} ± SD (µM) concentrations (NCI-SRB assay).

	Patient #1	**Carboplatin-Resistant OVSAHO**	**Olaparib-Resistant OVSAHO**	**Carboplatin-Resistant OVCAR-3**	**Olaparib-Resistant OVCAR-3**
MC013	5.5 ± 2	21 ± 0.2	16.9 ± 1.2	11 ± 0.5	14.3 ± 0.4
MC030	8.5 ±1	27.4 ± 1	27.3 ± 1.5	22.4 ± 1.1	22.7 ± 0.6
MC060	7 ±1.6	25.5 ± 1.3	21.7 ± 1.9	15.2 ± 6	17.7 ± 0.4
Carboplatin	<2.5	>200	N/A	8 µM ± 1.6	N/A
Cisplatin	<2.5	N/A	N/A	N/A	N/A
Olaparib	N/A	N/A	197 ± 4.4	NA	112.9 ± 6

Thus, based on the previous results obtained from the initial cytotoxicity screening and their further investigation, chalcone derivatives exhibiting promising efficacy against primary, chemo-resistant, and established ovarian cancer cells (MC013, MC030, MC060) were selected for further analysis, showing anti-cancer potential.

3.3 MC013, MC030, and MC060 effectively inhibit the colony-formation abilities of ovarian cancer cells

To further investigate the anti-proliferative properties of MC013, MC030, and MC060 on HGSOC cell lines, a colony-formation assay was performed for each compound respectively, for 24 h and 48 h time points. Considering the fact that cancer cells are prone to grow and proliferate by forming colonies, a clonogenic assay was performed to determine the effects of three selected derivatives on the capability of a single ovarian cancer cell to survive and grow into a colony (Franken et al., 2006).

HGSOC cell lines were treated with 1 µM, 2.5 uM, 5µM, and 10 uM concentrations of selected compounds or 0 µM (DMSO controls) for 24 h or 48 h. Changes in the colony formation ability of compound-treated cells compared to the controls are shown in Figure 3.2.

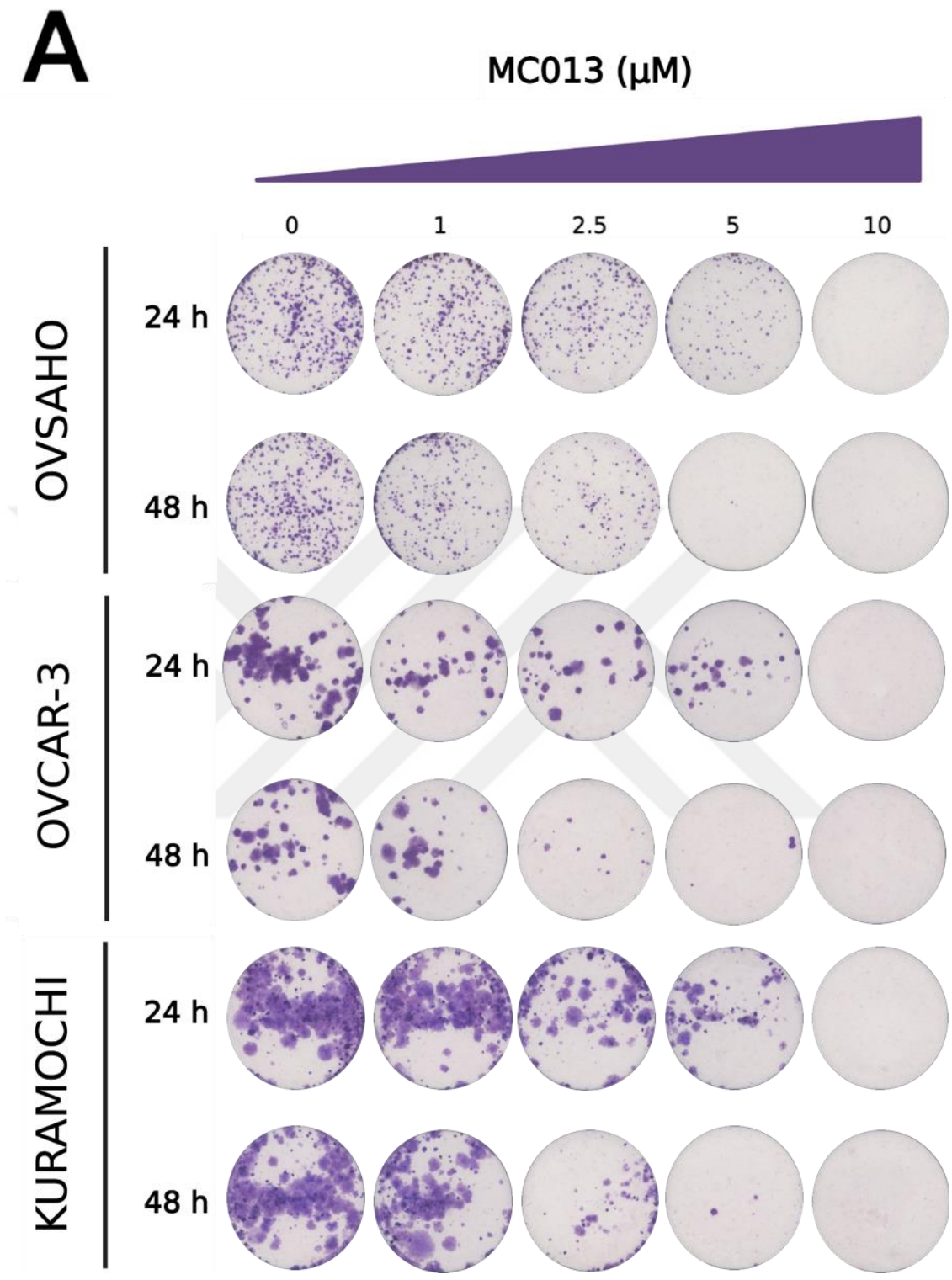
A
MC013 (µM)
0
1
2.5
5
10
OVSAHO
24 h
48 h
OVCAR-3
24 h
48 h
KURAMOCHI
24 h
48 h

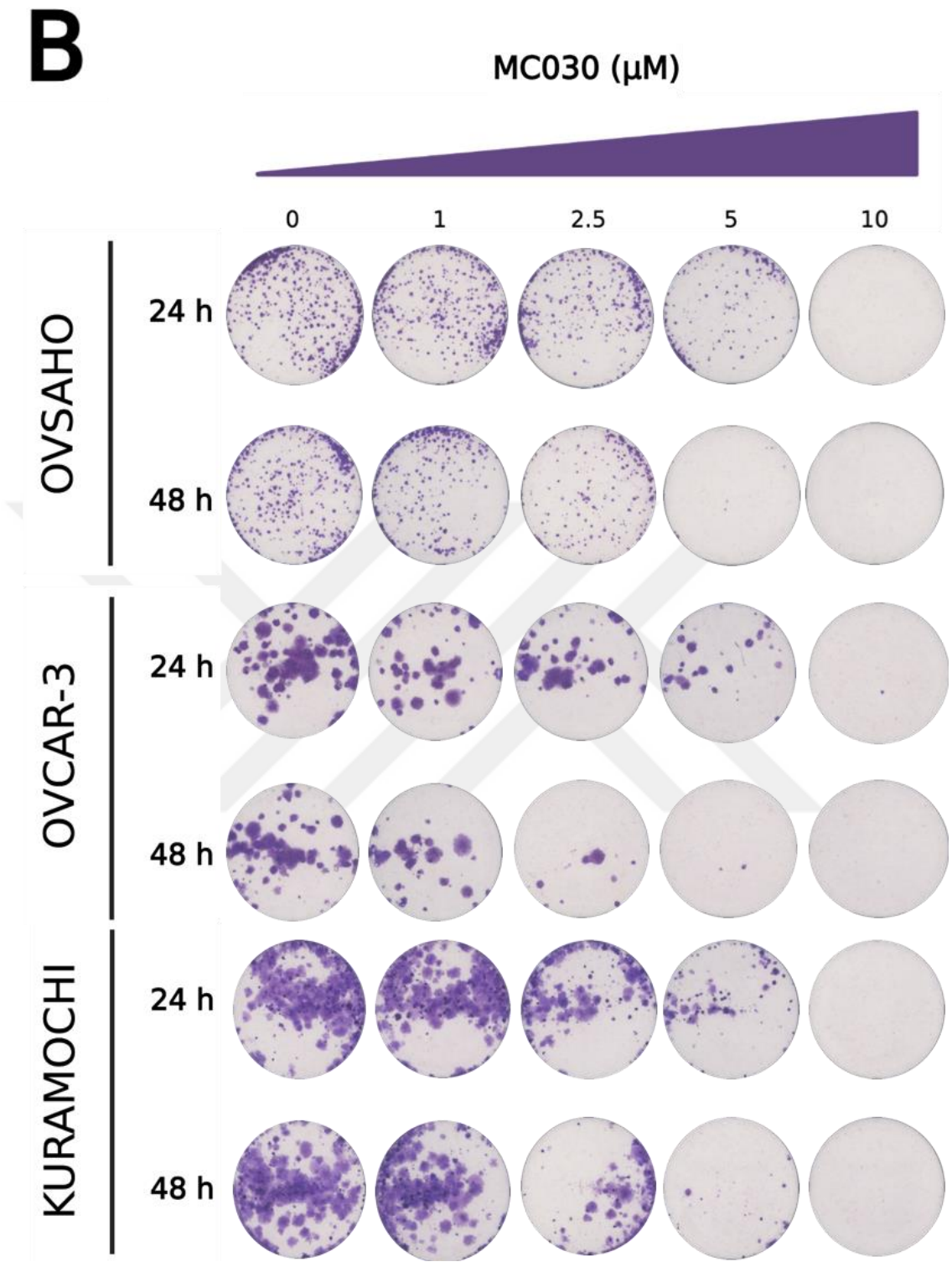
B
MC030 (µM)
0
1
2.5
5
10
OVSAHO
24 h
48 h
OVCAR-3
24 h
48 h
KURAMOCHI
24 h
48 h

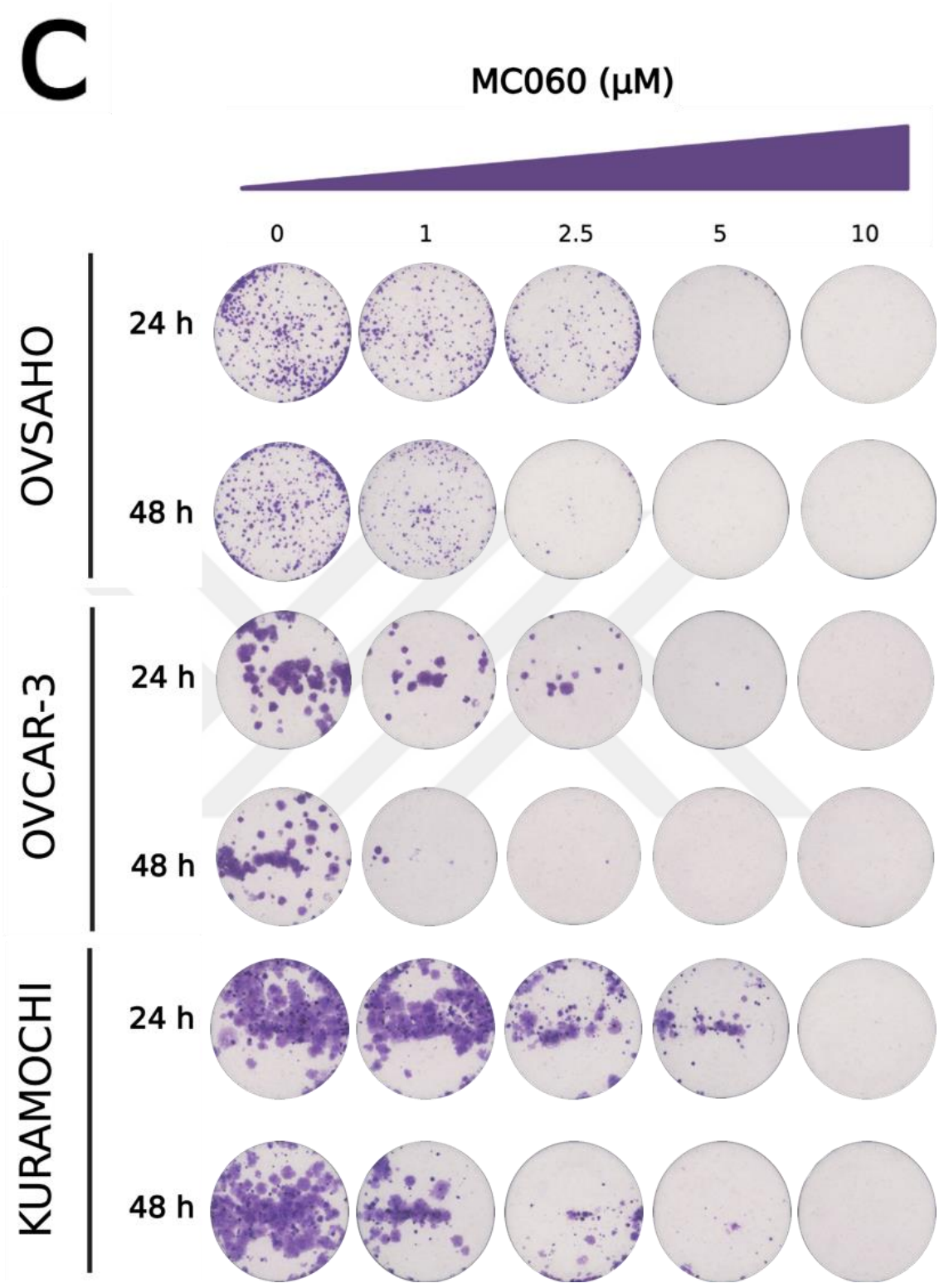

Figure 3.2: Long-term colony-formation assay of 3 HGSOC cell lines; O VSAHO, OVCAR-3, and KURAMOCHI after (A) MC013, (B) MC030, or (C) MC060 treatment. Cells were grown in the absence or presence of selected compounds at different concentrations for 16-21 days, fixed and stained with crystal violet.

Based on the data obtained (Figure 3.2), It was found that treatment with each three compounds decreased the colony numbers formed in all ovarian cancer cell lines in a dose-dependent manner respectively when compared to control cells. Besides, compounds inhibited the colony-formation ability of cancer cells in a time-dependent manner as well, showing a higher reduction in 48 h treatment than 24 h in all cell lines. While all selected compounds lead to a significant decrease in colony formation abilities of all cancer cells, especially MC060 reduced the number of colonies formed in both OVSAHO, OVCAR-3, and KURAMOCHI the most (Figure 3.2c). Moreover, no cell lines were observed to form colonies at compound doses of 10 µM at both 24h and 48 h. These data correlated with the results obtained previously with the SRB assay, showing that the selected derivatives have promising anti-proliferative effects on ovarian cancer cells.

3.4 Selected compounds modulate significant alterations in the cell cycle profiles of ovarian cancer cells

Cell cycle mechanism, which controls cell proliferation, is disrupted in cancer cells in almost every case, causing them to divide continuously and excessively (Matthews et al., 2022). In light of this information, the effects of selected chalcones on the cell cycle machinery of ovarian cancer cells were further investigated. For this purpose, propidium iodide (PI) staining method was performed. HGSOC cell lines were either treated with IC_{75} concentrations of selected compounds or DMSO controls for 48 h or 72 h periods and stained with red-fluorescent DNA-intercalating dye, propidium iodide. The cell cycle profiles of each cell line after treatment are shown in Figure 3.3. The results demonstrated that compound treatments caused major alterations in the cell cycle characteristics of ovarian cancer cells (Figure 3.3). All compounds induced the most significant changes in OVSAHO and OVCAR-3 cell lines at 48h time point respectively by leading to a significant increase in SubG1 cell populations, following the significant decrease in % of cells in G0/G1 phases (Figure 3.3B) At 48h time point, neither of the chalcones did show a significant alteration in the cell cycle distribution of KURAMOCHI cells. Furthermore, at 72h time point, MC030 and MC060 further caused a prominent increase in the SubG1 cell population of OVCAR-3 cells while their effect on the SubG1 phase did not prolong for OVSAHO cells. Regarding the compound treatment,

KURAMOCHI cells also had a slight increase in the % cells in the SubG1 phase of the cell cycle at 72h in contrast to their 48h cell cycle profile.

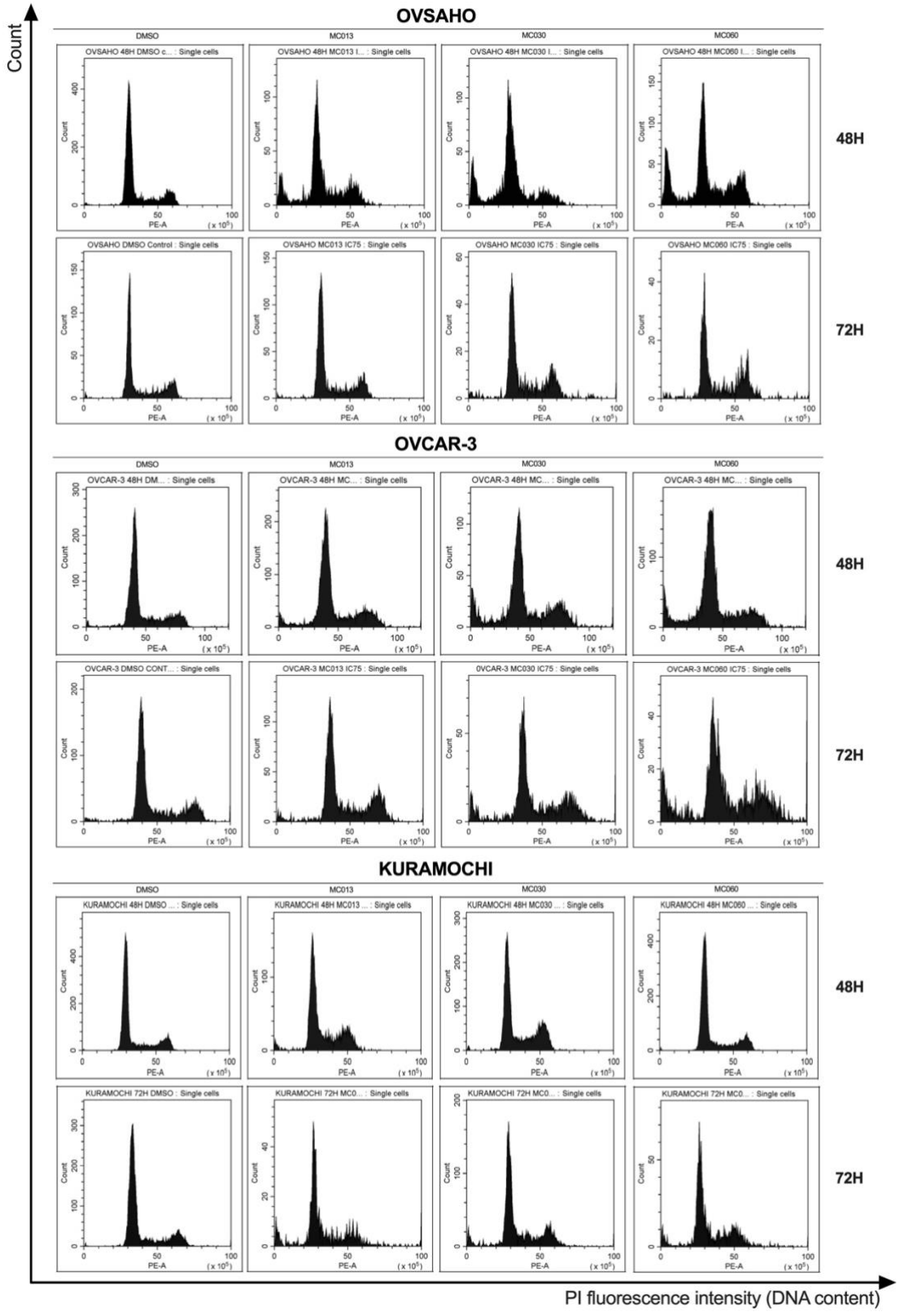

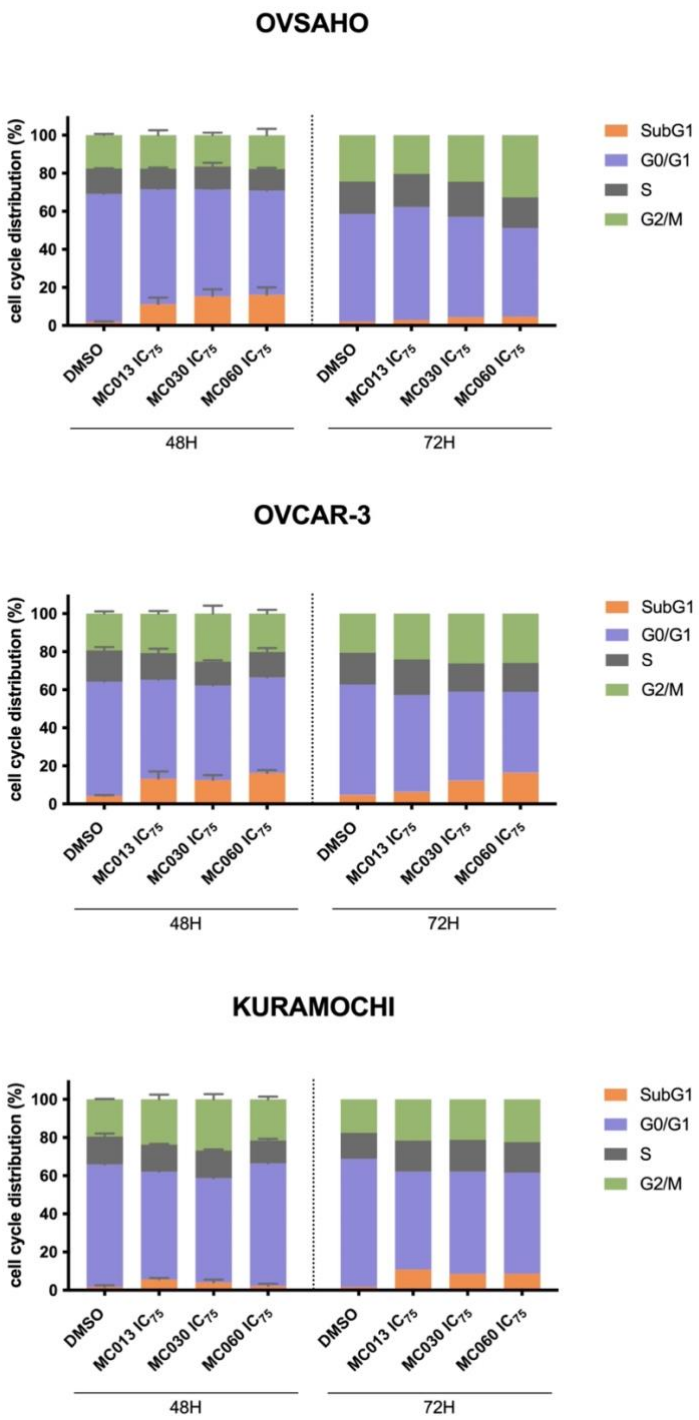

Figure 3.3: Cell cycle analysis of ovarian cancer cells. (A) Representative cell cycle histograms after PI staining. OVSAHO (top), OVCAR-3, (middle), and KURAMOCHI (bottom) cells were grown in the absence or presence of selected compounds at IC_{75} concentrations for 48h or 72h. The peak around 30-40 PE-A represents G0/G1 phase (2N); around 60-80 represents G2/M phase, and the area in between represents S phase. (B) The quantitation of cell cycle distribution analysis in bar graphs.

Therefore, these results suggested that MC013, MC030, and MC060 led to significant alterations in cell cycle profiles of OVCAR-3 and OVSAHO cells at 48h by inducing SubG1 arrest, which could occur as a result of apoptotic cell death. The promising apoptosis-inducing abilities of these selected compounds on OVSAHO and OVCAR-3 cells were further investigated.

3.5 MC013, MC030, and MC060 induced apoptotic cell death in OVSAHO and OVCAR-3 cells

After it was found that the selected molecules caused a significant increase in the SubG1 cell populations of OVSAHO and OVCAR-3 cells, it was decided to conduct a detailed investigation into whether the compounds cause apoptotic cell death. The sub-G1 phase of the cell cycle, which resides on the left side of the G0/G1 population, represents the fragmented DNA content lost from permeabilized cells as a result of cell death (Plesca et al., 2008). Since DNA fragmentation is one of the certain characteristics of apoptosis, our findings in cell cycle analysis suggested that selected chalcones might have acted on OVSAHO and OVCAR-3 cells through apoptosis induction (Matassov et al., 2004). To further define whether the cell viability decrease in ovarian cancer cells with the SubG1 increase was due to apoptotic cell death or another type of cell death such as necrosis, which also shows DNA lost profiles, Annexin-V/7-AAD double staining was performed. After OVSAHO and OVCAR-3 cells were treated with the compounds (IC_{75}) for 48h, the fraction of live, early apoptotic, late apoptotic, and dead cell populations were determined by MUSE cell analyzer (Figure 3.4).

Apoptosis results in some characteristic changes in the cell one of which is the phosphatidylserine (PS) externalization to the outer surface of the cell membrane. Annexin-V has a high-affinity binding for PS and therefore, annexin-V (+) populations demonstrate the externalization of phosphatidylserine, which is normally a component of the inner membrane of the cell, to the outer surface and its externalization used as an ongoing apoptosis marker. To selectively distinguish the apoptotic cells between dead cells, 7-AAD which is a fluorescent marker binding to DNA is also used as a dead cell marker (Vermes et al., 1995; Zembruski et al.,2012).

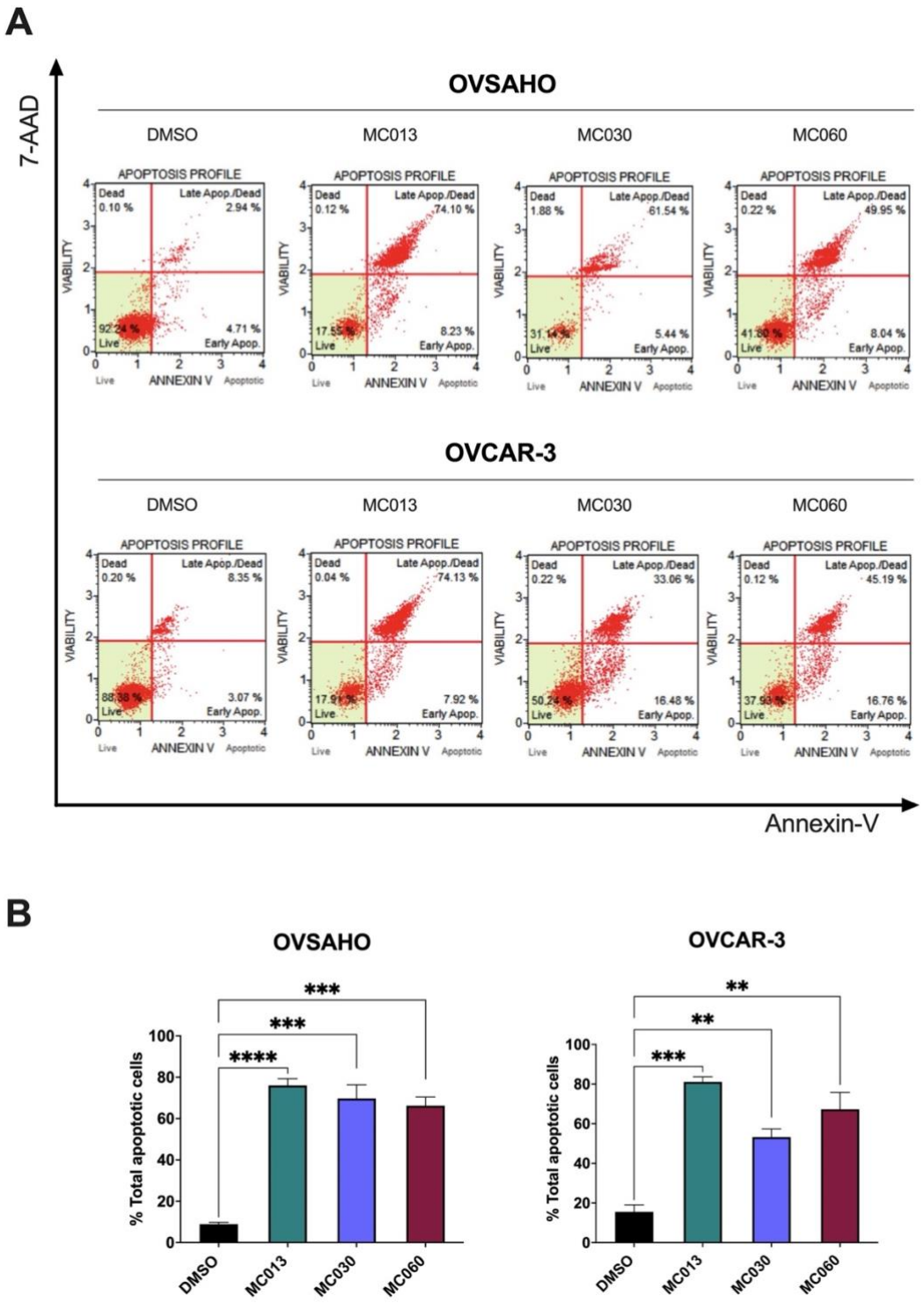

Figure 3.4: Apoptosis induction analysis of OVSAHO & OVCAR-3 cells after 48h compound treatment. (A) Representative plots of apoptosis profile. (B) The quantitation of analysis is presented on bar graphs. Error bars represent the SEM of data obtained in n=3 independent experiments; two-tailed Student's t-test in comparison to DMSO; ^{ns} p>0.05, * p<0.01, ** p<0.001, *** p<0.0001, **** p<00001.

In light of this information, MUSE Annexin-V & Death Cell assay demonstrated that live cells% in both OVSAHO and OVCAR-3 cells significantly decreased when treated with each compound respectively (Figure 3.4). At the same time, Annexin-V (+) cells increased to around 60-80% of the total cell population for samples treated with MC013, MC030, and MC060 respectively both in OVSAHO and OVCAR-3 cells while their corresponding controls did not have any significant Annexin-V (+) cell population as expected (Figure 3b). While all of the compounds significantly increased the total apoptotic cells in OVSAHO and OVCAR-3 cells, especially MC013 showed the most significant effect against ovarian cancer cells. In both cell lines, 48h exposure to each compound led to a potent increase in the late apoptotic cell populations (Annexin-V (+), 7-AAD (+)) with a slightly increased early apoptotic cell fractions (Annexin-V (+), 7-AAD (-)) (Figure 3a). Neither of the cell lines had Annexin-V (-) 7-AAD (+) cell populations (such as necrotic cell death), which proved that the selected chalcones induced apoptotic cell death. Thus, selected chalcones, MC013, MC030 and MC060, resulted a prominent decrease in cell viability and induced a significant apoptotic cell death in ovarian cancer cells, OVSAHO and OVCAR-3.

3.6 Selected chalcones effectively induced caspase-dependent apoptotic cell death through caspase-3/7 activation

To investigate the ability of selected chalcones to induce apoptosis on OVSAHO and OVCAR-3 cell lines in more detail, the MUSE Caspase-3/7 assay was performed for each compound for a 48h time point, respectively. With the aid of annexin-V/7-AAD double staining, chalcones were found to induce apoptosis in OVSAHO and OVCAR-3 cells at 48h, which correlated with the SubG1 increase in their cell cycle distributions. As a next step, it was decided to investigate the compounds' ability to activate caspase-3 and caspase-7. Caspase-3 and caspase-7 are proteases that play role in apoptosis as effector caspases. After initial pro-apoptotic signals come and apoptosis starts, effector caspases are activated and cleave important proteins in downstream pathways, by eventually promoting cell death. Thus, activation of caspase-3/7 is also one of the characteristic changes in the apoptosis process just like the externalization of phosphatidylserine (Elmore, 2007).

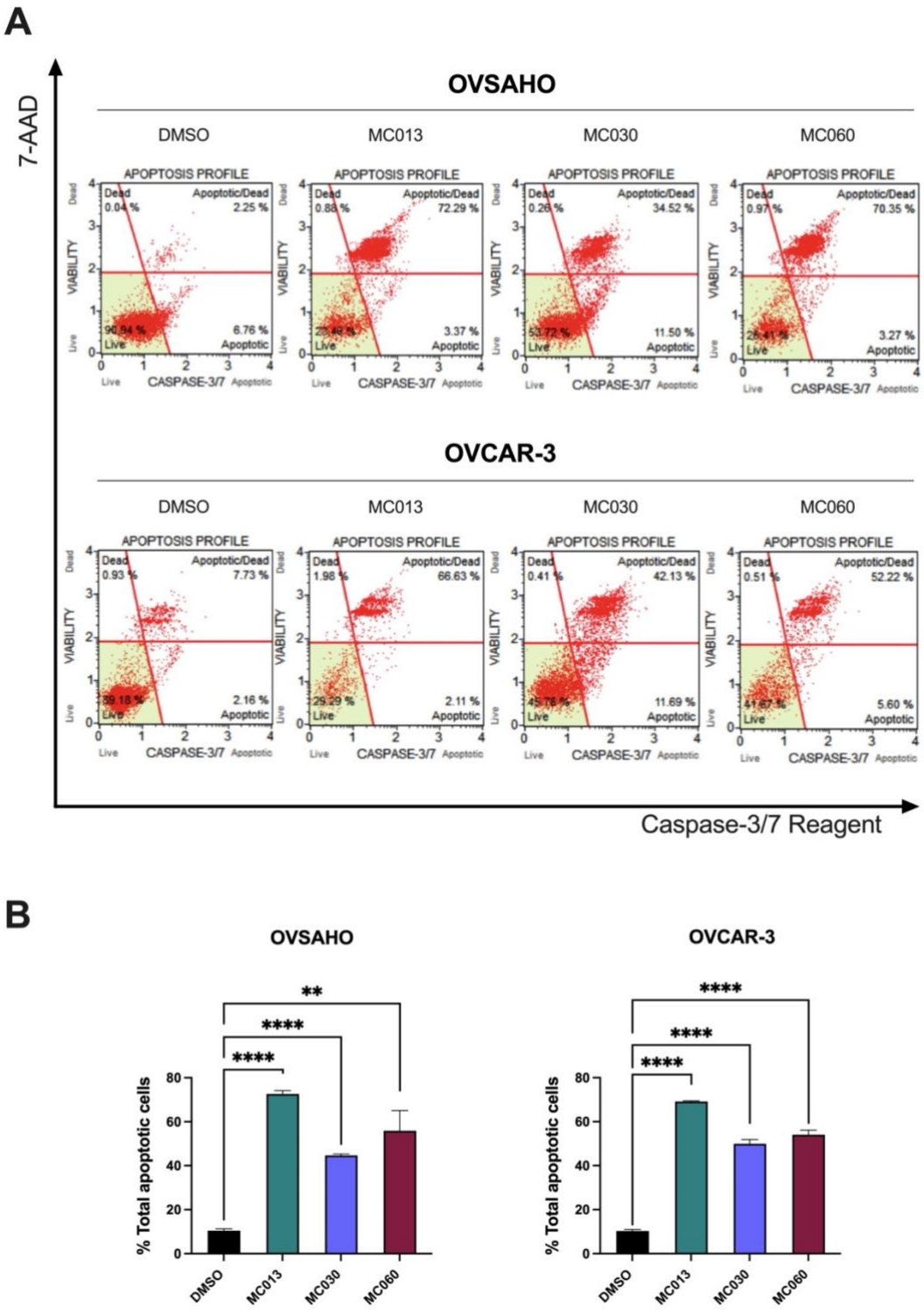

Figure 3.5: Caspase-3/7 activation analysis of OVSAHO & OVCAR-3 cells after 48h compound treatment. (A) Plots of the MUSE caspase-3/7 assay. (B) The quantitation of analysis is presented on bar graphs. Error bars demonstrate the SEM of data obtained in n=3 independent experiments. Statistical differences were analyzed with two-tailed Student's t-test in comparison to DMSO; ^{ns} $p>0.05$, * $p<0.01$, ** $p<0.001$, *** $p<0.0001$, **** $p<00001$.

The differences in the active/inactive Caspase-3/7 populations in OVSAHO and OVCAR-3 cells are demonstrated in Figure 3.5. The results confirmed the previous annexin-v & death cell assay findings and showed that MC013, MC030 and MC060 caused significant apoptosis induction (Figure 3.5). Besides, it also revealed that cell populations at where caspase-3 and caspase-7 are activated were significantly increased after each drug treatment respectively (Figure 3.5b). Correlated with the previous findings, late apoptotic cell populations were significantly higher and the early apoptotic cells were slightly increased. Neither of the cell lines had Caspase-3/7 Reagent (-) 7-AAD (+) cell populations which again proved that the selected chalcones induced apoptotic cell death rather than necrosis. Since the total apoptotic cells% were mostly similar to total caspase3-7 activation% in both cell lines, it was concluded that selected chalcones induced caspase-dependent apoptotic pathway in ovarian cancer cells, OVSAHO and OVCAR-3.

3.7 MC013, MC030, and MC060 target ovarian cancer cells via inducing DNA damage

Considering the previous findings in the literature that some anti-cancer drugs induce DNA damage, DNA damage accumulation after chalcone treatment was investigated in ovarian cancer cells (Reuvers et al., 2020).

When cells are exposed to a DNA damage-inducing agent, double-strand breaks may form and could lead to several deficiencies if they are left unrepaired including genomic instability, cell survival, or cancer. The cells then activate their DNA damage response mechanisms to repair the damage. As one of the steps in this activation process, phosphorylation of the histone variant H2A.X to γH2AX has a crucial role in the DNA damage response mechanism. Thus, the increased γH2AX levels in the cells are used as a DNA damage marker, as a result of double-strand breaks (Reuvers et al., 2020; Podhorecka et al., 2010).

To be able to investigate the DNA-damage-inducing capabilities of chalcone compounds, OVCAR-3 cells were treated with MC013, MC030, or MC060 (IC_{75}) for 48h respectively. Cells were then incubated with phospho-Histone H2A.X primary antibody

conjugated with Alexa Fluor 594 secondary antibody (red) and visualized by confocal microscopy. The nuclei were stained with DAPI (blue). The differences in γH2AX levels between chalcone-treated and control cells are demonstrated in Figure 3.6 below.

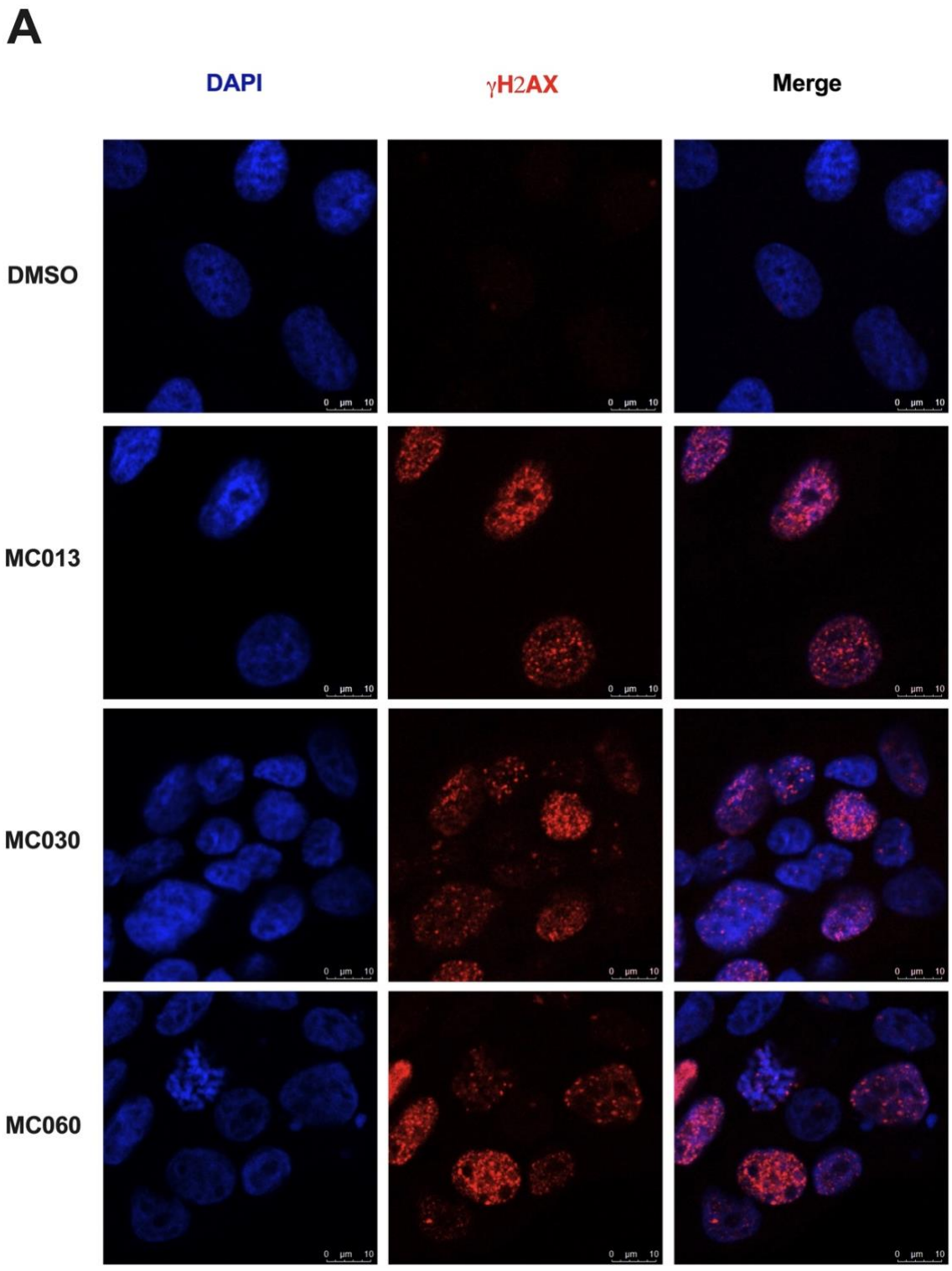

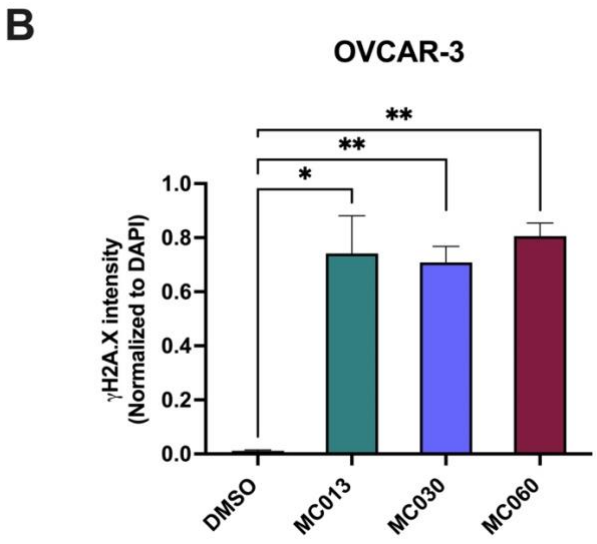

Figure 3.6: Detection and quantification of γH2A.X levels using immunofluorescence assay. (A) Representative fluorescent images of γH2A.X staining after 48h compound exposures of OVCAR-3 cells (Scale bar: 10µm) (Blue: DAPI, Red: γH2A.X). (B) The quantitation of changes in γH2A.X levels is presented on bar graphs. γH2A.X intensities were normalized to DAPI. Error bars represent the SD of data and statistical differences were analyzed with two-tailed Student's t-test in comparison to DMSO.

All selected chalcones were shown to induce a significant increase in γH2A.X levels in OVCAR-3 cells respectively, which was the main indicator of DNA damage increase (Figure 3.6). No change in DMSO control was observed as expected. As a result, after 48h exposure to either of the selected chalcones, OVCAR-3 cells had prominent DNA damage, proving that chalcones act on OVCAR-3 cells via DNA damage.

3.8 MC013, MC030, and MC060 deregulates several apoptosis-related proteins

Based on our previous data, selected chalcones were shown to have significant effects on the cell cycle, apoptosis, and DNA damage profiles of ovarian cancer cells. To further characterize the possible molecular mechanisms which are responsible for their apoptosis-inducing action in ovarian cancer cells, the expression levels of apoptosis-related proteins were determined by performing a western blot analysis. OVCAR-3 cells

were treated with the corresponding MC013, MC030, and MC060 concentrations (IC_{75}) for 48h, proteins were isolated and protein levels were investigated through western blot (Figure 3.7a).

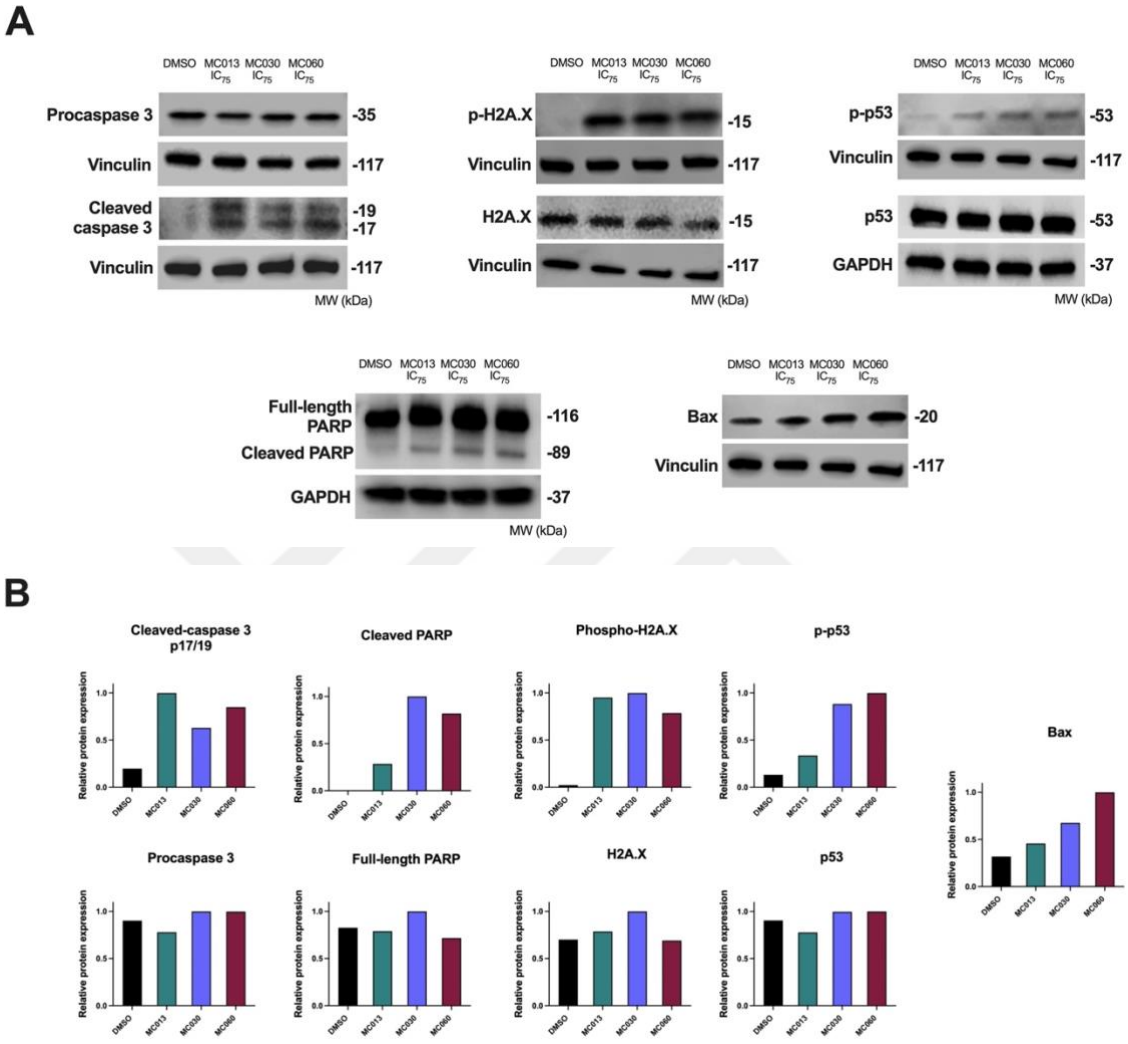

Figure 3.7: Apoptosis-related proteins targeted by selected chalcones. (A) Representative images of blots. (B) The quantitation of changes protein levels is presented on bar graphs. Images were quantified using ImageJ software.

To confirm the caspase-3/7 activation assay results which demonstrated the increase in the activated caspase-3 levels in the ovarian cancer cells after chalcone treatment, caspase-3 changes were measured at protein level this time. It was found that for each treatment, the expression of the cleaved forms of caspase-3 (17-19kDa) was

significantly increased in OVCAR-3 cells while their corresponding full-length caspase-3 expression did not change (Figure 3.7). Since the cleavage of full-length caspases to their cleaved forms lead to their activation, the significant increase in the cleaved caspase-3 levels in OVCAR-3 cells demonstrated that chalcones induced apoptosis through the activation of the caspase cascade. In the next step, full-length and cleaved poly (ADP-ribose) polymerase-1 (PARP-1) expression levels were also measured to see if PARP-1 cleavage, which is an indicator of apoptosis, was induced as a result of effector caspase-3 activation (Chaitanya et al., 2010). It was revealed that cleaved PARP-1 (89 kDa) levels in OVCAR-3 cells were significantly increased compared to the control after being exposed to selected chalcones respectively (Figure 3.7b). Thus, downstream cleavage of PARP-1 after caspase cascade activation confirmed that caspase-mediated apoptosis was induced in OVCAR-3 cells.

In the literature, it was demonstrated that cellular stresses such as DNA damage can induce apoptosis (De Zio et al., 2013). In the previous results, we found that selected chalcones stimulated DNA damage in OVCAR-3 cells with the aid of the immunofluorescence protocol, which showed increased levels of γH2A.X. To confirm the increased γH2A.X expression, its expression was also measured at the protein level by western blot. As a result of 48h exposure to each chalcone, phosphorylated H2A.X levels in OVCAR-3 cells were significantly increased in OVCAR-3 cells, correlated with the previous findings (Figure 3.6) (Figure 3.7). This finding also prompted us to investigate whether there are any changes in the levels of the p53, which is stimulated in response to cellular stresses such as DNA damage, which can restrict cell division throughout the cell cycle and also induce apoptosis (Ozaki & Nakagawara, 2011). Western blot analysis revealed that along with the increase in γH2A.X, selected chalcones induced the phosphorylation of p53 in OVCAR-3 cells, which meant the activation of p53 (Figure 3.7). Thus, our findings demonstrated that p53 (tumor suppressor) was activated in OVCAR-3 cells as a response to DNA damage caused by chalcones and could be the regulator of downstream apoptosis mechanism.

To characterize the downstream regulatory effects of p53 and to further investigate which apoptotic pathway was induced after chalcone treatment, the expression levels of proapoptotic protein Bax were measured. In the literature, it was shown that p53

has a role as an upstream regulator of proapoptotic protein Bax, whose translocation from cytosol to outer membrane of mitochondria plays a significant role in p53-induced and mitochondria-dependent apoptosis and is an initial step for caspase activation (Chipuk et al., 2004). Western blot analysis of Bax revealed that there was a significant increase in Bax levels in OVCAR-3 after compound treatment especially with MC030 and MC060, which was compatible with the information in the literature (Figure 3.7b).

3.9 Selected chalcones stimulated cell cycle arrest in OVCAR-3 cells through cyclin D1 down-regulation

Cyclin D1 is a cell cycle regulatory protein that is important in cell cycle progression through the G1 phase of the cycle. Its overexpression is linked to tumor growth and cancer progression and seen in many cancer types (Qie & Diehl, 2016). Our findings in PI staining prompted us to further investigate the cell cycle characteristics of OVCAR-3 cells after chalcone treatment. As a result of the PI staining experiment, it was observed that chalcone molecules had a significant effect on the cell cycle profiles of ovarian cancer cells and caused subG1 arrest (Figure 3.3). In addition, it was previously mentioned that the activation of p53 protein after DNA damage may cause cell cycle arrest. In line with this information, it was desired both to confirm the results obtained from PI staining and to measure the expression levels of cyclin D1 regulated by the p53 protein, which has an important role in the cell cycle.

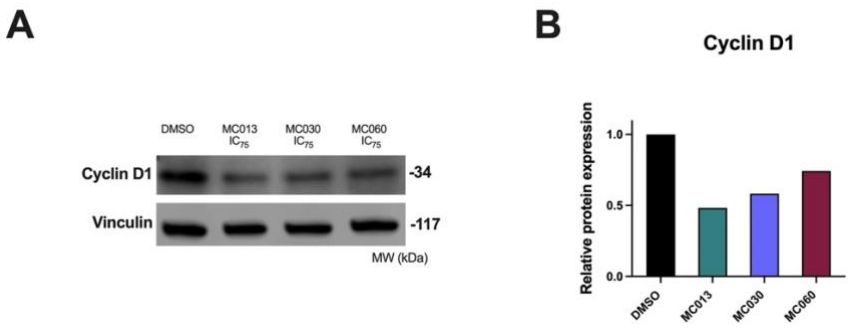

Figure 3.8: Cyclin D1 protein levels in OVCAR-3 cells after chalcone treatment. (A) demonstrates the representative blot images of cyclin D1 and its housekeeping control protein, vinculin. (B) The quantitation of cyclin D1 levels are in bar graphs. Images were analized using ImageJ software.

Western blot analysis demonstrated that 48h treatment with chalcone compounds respectively led to a significant decrease in cyclin D1 levels in OVCAR-3 cells compared to the control, especially after MC013 and MC030 treatment (Figure 3.8). This result suggested that p53 could be responsible for the downregulation of cyclin D1, which resulted in cell cycle arrest correlated with our previous findings.

3.10 MC013 slighlty decreased Akt phosphorylation in OVCAR-3 cells

In several studies in the literature on the mechanism of action of synthetic chalcones, it was shown that chalcones act via the PI3K/Akt pathway (Sahin et al., 2020; Noser et al., 2022) On the other hand, PI3K/AKT signaling pathway is one of the key altered pathways identified in HGSOC, which is hyperactivated in a majority of cases (Dobbin & Landen, 2013). In light of this information, activation of Akt was investigated through phosphorylated Akt expression levels by western blot. Results revealed that among selected molecules MC013 caused a slight decrease in phosphorylated Akt levels in the OVCAR-3 cells, which suggested that chalcone treatment might have an impact on PI3K/Akt pathway by decreasing hyperactivated p-Akt levels (Figure 3.9).

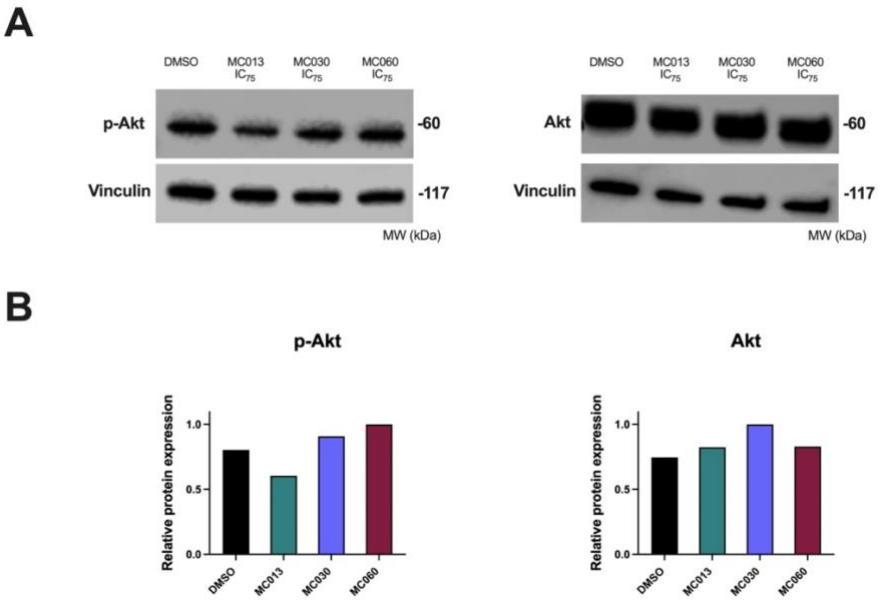

Figure 3.9: Investigation of akt phosphorylation in OVCAR-3 cells after chalcone treatment. (A) Representative blot images. (B) Band analysis was demonstrated in bar graphs.

3.11 MC013, MC030, and MC060 might have a significant effect on epithelial-mesenchymal transition (EMT) mechanism

Epithelial-mesenchymal transition is an important mechanism in tumorigenesis by increasing migratory and metastatic properties of tumor cells. It is represented by lower E-cadherin levels and higher N-cadherin expression (Micalizzi et al., 2010). Thus, to investigate whether the selected chalcones show any effect on EMT mechanisms on ovarian cancer cells, E-cadherin expression levels were measured. Western blot analysis revealed that E-cadherin levels significantly increased in OVCAR-3 cells treated with each chalcone respectively while DMSO still had the low level of E-cadherin expression (Figure 3.10). This suggested that selected chalcones may act on EMT pathway in OVCAR-3 cells and decrease their migratory and invasive properties as a result of the E-cadherin increase.

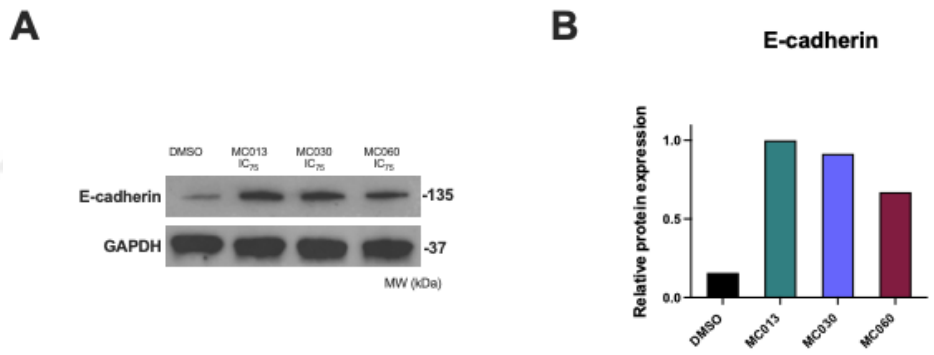

Figure 3.10: Quantification of e-cadherin levels in OVCAR-3 cells by western blot. (A) Representative blot images showing the E-cadherin increased induced by selected chalcones. (B) Relative protein expression was in bar graph. Band intensities were measured using ImageJ software by normalizing to equal loading control GAPDH.

3.12 MC013 and carboplatin have no synergistic effect on carboplatin-resistant OVCAR-3 cells

Based on our previous results, it was revealed that selected chalcones act on ovarian cancer cells through cell cycle arrest, apoptosis induction, and DNA damage.

Since these molecules demonstrated promising anti-cancer effects on carboplatin-resistant OVCAR-3 cells as well (Table 3.3), these abilities of chalcones prompted us to question if they synergistically act with carboplatin on carboplatin-resistant OVCAR-3 cells. For this, MC013, which showed the most promising effect on carboplatin-resistant OVCAR-3 cells with a low IC_{50} profile, was chosen for testing. Carboplatin-resistant OVCAR-3 cells were either treated with increasing concentrations of MC013 (0 µM, 2.5 µM, 5µM, and 10µM), carboplatin (0 µM, 5µM, 10µM, 20µM, and 40 µM) or both for 72 h. After 72h, the inhibition effects were calculated as percentages (Table 3.4). The combination index data revealed that MC013 and carboplatin had no combinational effect on resistant cells (Table 3.5).

Table 3.4: Growth inhibition % for the combinational treatment of MC013 and carboplatin on carboplatin-resistant OVCAR-3 cells.

Carboplatin-Resistant OVCAR-3						
		Carboplatin				
		40 µM	**20 µM**	**10 µM**	**5µM**	**0 µM**
MC013	**10 µM**	90.56	82.73	78.11	74.83	60.67
	5 µM	87.95	74.82	56.33	42.84	57.70
	2.5 µM	90.38	77.58	59.56	37.33	35.51
	0 µM	88.23	66.12	53.01	41.71	25.63

Table 3.5: Combination index values for the combinational treatment of MC013 and carboplatin on carboplatin-resistant OVCAR-3 cells.

Carboplatin-Resistant OVCAR-3						
		Carboplatin				
		40 µM	**20 µM**	**10 µM**	**5µM**	**0 µM**
MC013	**10 µM**	1.05	1.05	1.04	1.03	1.17
	5 µM	1.08	1.15	1.42	1.76	1.19
	2.5 µM	1.02	1.01	1.17	1.67	1.47
	0 µM	1.03	1.13	1.23	1.36	1.74

Chapter 4:
DISCUSSION

High-grade serous ovarian carcinoma is the most common epithelial ovarian cancer in women and also the deadliest one, characterized by limited treatment options and a high mortality rate. Due to its chemoresistance profile and poor response to conventional chemotherapy, it is essential to come up with new treatment options for the treatment of HGSOC (Bowtell et al., 2015; Jayson et al., 2014). With this aim, the discovery of new drugs that might be used in HGSOC therapy has gained great importance.

In the literature, chalcones extracted from several medicinal plants were shown to have cytotoxic and anti-cancer activities against several tumor types at nM or µM concentrations (Constantinescu & Lungu, 2021; Constantinescu & Mihis, 2022). Besides, most of the studies revealed that chalcones are easy to synthesize in the lab and the modification of their main structure, which provides their activity, is also easy. In this thesis, cytotoxic activities of newly synthesized 16 chalcone molecules (synthesized by Michael Christodoulou and his research team at the University of Milano) were investigated on human ovarian cancer cells. Their action on proliferation, cell cycle distribution, colony formation ability, apoptosis profile, and DNA damage response of ovarian cancer cells was further determined. Our main aim was to identify and characterize novel chalcones that might be used as small-molecule inhibitors against ovarian cancer. Accordingly, cell viability assay, cell cycle analysis, apoptosis assay, caspase3-7 activation assay, DNA damage analysis through immunofluorescence, and western blot analysis were performed to investigate their anticancer activity. Therefore, as a result of these several investigations, we found out that especially 3 compounds among all 16 chalcones demonstrated promising anticancer activities against primary, carboplatin/olaparib-resistant, and established ovarian cancer cell lines, which proves that further research is required.

Throughout this project, firstly, the cytotoxic activity of novel 16 synthetic chalcones was investigated against a panel of four cell lines; three of them established

HGSOC cells and one of them was a breast normal epithelial cell line. As shown in Table 3.1, MC013, MC030, and MC060 (Figure 4.1) showed strong cytotoxic activity against ovarian cancer cells at mostly 10 µM concentrations while they were less cytotoxic to breast normal epithelial cells, which makes them promising molecules as anti-cancer therapeutics since any harm to normal cells is not be desired for targeted small molecule inhibitors (Padma, 2015). Two of the chalcones were not cytotoxic to any of the cell lines while the other 11 molecules were either effective to only one of the cell lines or not. This data confirms that chalcones are easily modified and their anti-cancer activities can be improved through structural changes as shown for MC013, MC030, and MC060.

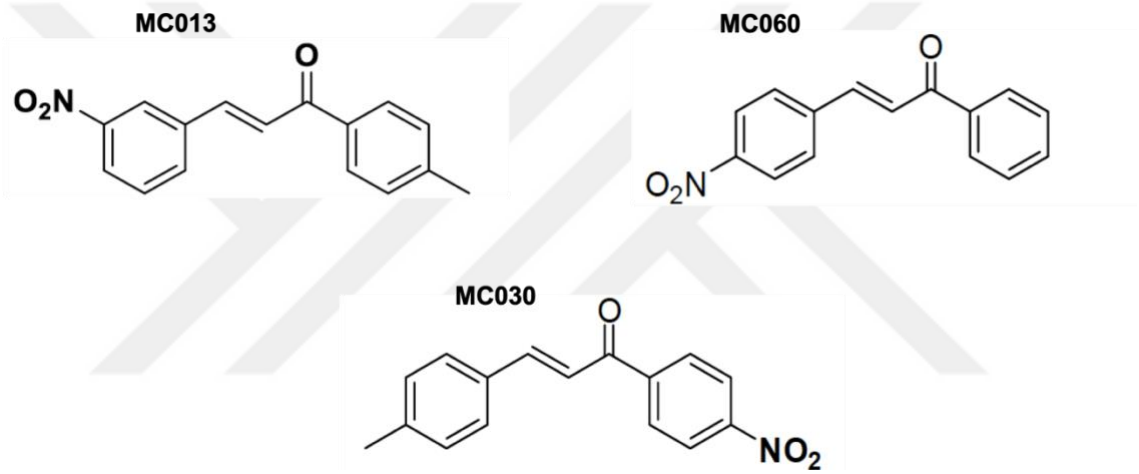

Figure 4.1: Chemical structures of MC013, MC030, and MC060.

Since MC013, MC030, and MC060 showed potent anti-proliferative activity against high-grade serous ovarian cancer cells, their activities were further tested on an enlarged panel of ovarian cancer cells consisting of primary cells obtained from a patient diagnosed with HGSOC and chemoresistance ovarian cancer cell lines established in our lab. As shown in Table 3.3, these selected compounds demonstrated high cytotoxicity around 10-20 µM concentrations again but this time to ovarian cancer cells that were more clinically relevant with their chemoresistance behavior and patient-derived profiles. These results confirmed that their anti-proliferative activities and potential as anticancer

therapeutics were high against several types of ovarian cancer cells with different origins, thus they were selected for further investigation.

To further investigate the anti-proliferative activities of MC013, MC030, and MC060 on HGSOC cells, a clonogenic assay was performed. Colony formation analysis demonstrated that all 3 compounds significantly decrease the colony-formation abilities of ovarian cancer cells in a dose and time-dependent manner. This data correlates with our previous results showing their growth-inhibitory effects and also emphasizes the promising role of selected chalcones as anti-cancer molecules. To further determine their mechanism of action, the cell cycle profiles of ovarian cancer cells after each chalcone treatment were observed. Cell cycle analysis through PI staining revealed SubG1/G1 cell cycle arrest by selected chalcones in OVCAR-3 and OVSAHO ovarian cancer cell lines especially at 48h time point, which supports the idea that these molecules induce apoptosis in ovarian cancer cells. Cell cycle machinery is important for cells to control their growth potential and any change in this mechanism may cause cells to proliferate continuously, leading to several disorders including cancer. Cancer cells are characterized by disrupted cell cycle mechanisms resulting in their continuous growth (Otto & Sicinski, 2017). Thus, the development of drugs playing roles in the cell cycle and prevent the impaired cell cycle mechanisms of cancerous cells is very important in cancer therapies (Bai et al., 2017). For instance, one of these drugs, paclitaxel, is one of the chemotherapeutic drugs that is used in the first-line standard therapy for ovarian cancer with platinum-based drugs. At high doses, it acts on the cell cycle through G2/M arrest and prevents cell proliferation by eventually leading to apoptosis. At low doses, instead, it induces apoptosis at G0/G1 phases (Kampan et al., 2015). Thus, in light of this information, the effects of our selected molecules on the cell cycle of ovarian cancer cells by leading to SubG1/G1 arrest confirmed their promising role as anti-cancer agents and it was a significant finding to further investigate their anticancer properties and their role in apoptosis induction of ovarian cancer cells. According to the findings we obtained during the cell cycle analysis, the investigation of possible apoptosis induction of selected molecules in OVCAR-3 and OVSAHO cells was decided. For this, MUSE Annexin-V & Cell Death apoptosis assay was performed. The results revealed that all selected compounds significantly increased the number of total apoptotic cells in OVSAHO and OVCAR-3 compared to DMSO controls. These findings were correlated with the cell

cycle analysis results and confirmed that selected chalcones induced cell death in high-grade ovarian cancer cells through apoptosis. As a next step, the apoptotic pathway the compounds act on was determined by analyzing the differences in the active/inactive Caspase-3/7 populations in OVSAHO and OVCAR-3 cells. The results confirmed the previous findings and showed that MC013, MC030 and, MC060 caused significant apoptosis induction. Besides, caspase-3/7 activated cell populations were found to be significantly increased after each chalcone treatment compared to DMSO controls, which suggested that selected chalcones induced caspase-dependent apoptotic pathway in OVCAR-3 and OVSAHO cells. Previous findings revealed that some synthetic chalcones induced DNA damage in cancer cells by leading to the activation of stress-induced apoptosis (Singh et al., 2014). Based on this information, we decided to investigate the ability of selected chalcones to induce DNA damage in ovarian cancer cells and chose OVCAR-3 as a model cell line against which selected chalcones showed higher cytotoxic activity. Our results demonstrated that each of the chalcones significantly stimulated DNA damage in OVCAR-3 cells respectively. All of these findings prompted us to identify possible downstream signaling pathways which were targeted by chalcones. By performing western blotting, changes in protein levels associated with apoptosis were firstly investigated. Western blot analysis revealed that chalcones deregulated several apoptosis-related proteins in OVCAR-3 cells, confirming their apoptosis induction. Our results suggested that chalcone treatment induced caspase-3 and PARP-1 cleavage in OVCAR-3 cells, which is a certain hallmark of apoptosis. After an initial signal comes telling the cell to go through apoptosis, initiator caspases such as caspase-8 or caspase-9 activate downstream signaling cascades and eventually activate the effector caspases, caspase-3 and caspase-7 by inducing their cleavage. Their activation also induces the cleavage of PARP-1 and eventually results in apoptosis (Mcllwain et al., 2013; Chainya et al., 2010). Thus, our results proved the apoptotic effects of selected chalcones at the protein levels as well and also correlated with the previous results obtained from Annexin-V and Caspase-3/7 apoptotic assays. We also confirmed the DNA damage induced by chalcones by western blotting. Increased levels of γH2A.X in OVCAR-3 cells treated with chalcones also prompted us to investigate whether there were any changes in the tumor suppressor protein p53 levels, which is the main regulator of stress-induced apoptosis mechanisms (p53-induced apoptosis). The results revealed that OVCAR-3 cells treated with selected chalcones demonstrated an increase in phosphorylated p53 (active

p53) and Bax levels, and a decrease in CyclinD1 levels. Our findings suggested that as a response to chalcone treatment, cellular stress and DNA damage were induced in OVCAR-3 cells and possibly with the other stress-induced regulatory proteins (DNA damage response), p53 (tumor suppressor) was activated as a response to this change. In the literature, it was indicated that p53 has a role as an upstream regulator of Bax (Chipuk et al., 2004). Based on this information and our results demonstrating Bax increase, in OVCAR-3 cells, activated p53 possibly upregulated proapoptotic protein Bax which has an important part in the mitochondria-dependent apoptosis pathway (Wang & Youle, 2009). Its upregulation induced its translocation from cytosol to the outer membrane of mitochondria, which was a stimulator of downstream signaling cascades resulting in the cleavage of caspase-3/7 first followed by the cleavage of PARP-1 as a last step (Finucane et al., 1999). Meanwhile, activated p53 possibly downregulated cyclinD1, which is a cell cycle regulatory protein and its deactivation resulted in SubG1/G1 cell cycle arrest eventually causing apoptosis (Williams & Schumacher, 2016). This suggested mechanism of action for selected chalcones was confirmed in this study by cell cycle analysis, apoptosis assays, immunofluorescence, and western blot analysis. In addition to this, chalcones were previously shown to act via the Akt pathway (Sahin et al., 2020). In addition to this, PI3K/Akt signaling pathway is one of the main altered pathways characterized in HGSOC, which is hyperactivated in a majority of cases. Its activation promotes cellular survival and growth in cancer cells (Dobbin & Landen, 2013; Gasparri et al., 2017). In light of this, the phosphorylated Akt levels in chalcone-treated OVCAR-3 cells were investigated. Western results revealed that while there was no significant change in p-Akt levels for MC030 and MC013-treated cells, p-Akt decrease in MC013-treated OVCAR-3 cells was observed. This suggested that MC013 molecule might decrease the hyperactivation of Akt in OVCAR-3 cells, resulting in the prevention of cellular survival. As a last step, the effects of chalcones on the epithelial-mesenchymal transition mechanism (EMT) in OVCAR-3 cells, which play an important role in tumorigenesis, were investigated (Dudas et al., 2020). It is identified by decreased e-cadherin levels and increased n-cadherin levels (Gravdal et al., 2007). Western blot analysis revealed that e-cadherin levels in chalcone-treated OVCAR-3 cells were significantly increased. This could be a preliminary result whose further investigation is required, which might show that MC013, MC030, and MC060 act on the EMT pathway in OVCAR-3 cells by reversing its function back and decreasing their migratory potential.

CONCLUSION

In the present study, novel chalcone molecules MC013, MC030, and MC060 were identified as promising anti-cancer agents against high-grade serous ovarian cancer. These promising results require further investigation and characterization of these chalcones as therapeutic agents for ovarian carcinoma.

After the confirmation of apoptosis induction by these chalcones and the investigation of their mechanism of action in ovarian cancer cells, their upstream action mechanisms remain to be elucidated. The results demonstrate that chalcones have important activity against cancer cells. However, further experiments including wound healing, ROS assay, and *in vivo* experiments on ovarian cancer xenograft models are necessary to confirm their anticancer properties.

Overall, this thesis gives primary information about the potential of novel chalcone compounds as promising therapeutic agents in ovarian cancer treatment.

BIBLIOGRAPHY

Abbas, T., & Dutta, A. (2009). p21 in cancer: intricate networks and multiple activities. *Nature reviews. Cancer*, *9*(6), 400–414. https://doi.org/10.1038/nrc2657

Abdollahi, M., Jasamai, M., & Jantan, I. (2012). Synthesis and Biological Evaluation of chalcone Derivatives (Mini Review). *Mini-reviews in Medicinal Chemistry*, 12(13) 1394–1403. https://doi.org/10.2174/138955712804586648

Ashraf, R., Hamidullah, Hasanain, M., Pandey, P. C., Maheshwari, M., Singh, L., Siddiqui, M. M., Konwar, R., Sashidhara, K. V., & Sarkar, J. (2017). Coumarin-chalcone hybrid instigates DNA damage by minor groove binding and stabilizes p53 through post translational modifications. *Scientific Reports*, *7*(1). https://doi.org/10.1038/srep45287

Bai, J., Li, Y., & Zhang, G. (2017). Cell cycle regulation and anticancer drug discovery. *Cancer biology & medicine*, *14*(4), 348–362. https://doi.org/10.20892/j.issn.2095-3941.2017.0033

Bast, R. C., Jr, Hennessy, B., & Mills, G. B. (2009). The biology of ovarian cancer: new opportunities for translation. *Nature reviews. Cancer*, *9*(6), 415–428. https://doi.org/10.1038/nrc2644

Bowtell, D. D., Böhm, S., Ahmed, A. A., Aspuria, P. J., Bast, R. C., Jr, Beral, V., Berek, J. S., Birrer, M. J., Blagden, S., Bookman, M. A., Brenton, J. D., Chiappinelli, K. B., Martins, F. C., Coukos, G., Drapkin, R., Edmondson, R., Fotopoulou, C., Gabra, H., Galon, J., Gourley, C., … Balkwill, F. R. (2015). Rethinking ovarian cancer II: reducing mortality from high-grade serous ovarian cancer. *Nature reviews. Cancer*, *15*(11), 668–679. https://doi.org/10.1038/nrc4019

Cancer Genome Atlas Research Network (2011). Integrated genomic analyses of ovarian carcinoma. *Nature*, *474*(7353), 609–615. https://doi.org/10.1038/nature10166

Chaitanya, G. V., Steven, A. J., & Babu, P. P. (2010). PARP-1 cleavage fragments: signatures of cell-death proteases in neurodegeneration. *Cell communication and signaling: CCS*, *8*, 31. https://doi.org/10.1186/1478-811X-8-31

Champelovier, P., Chauchet, X., Hazane-Puch, F., Vergnaud, S., Garrel, C., Laporte, F., Boutonnat, J., & Boumendjel, A. (2013). Cellular and molecular mechanisms activating the cell death processes by chalcones: Critical structural effects. *Toxicology in vitro: an international journal published in association with BIBRA*, *27*(8), 2305–2315.

Chen, C., Huang, S., Chen, C. L., Su, S. B., & Fang, D. D. (2019). Isoliquiritigenin Inhibits Ovarian Cancer Metastasis by Reversing Epithelial-to-Mesenchymal Transition. *Molecules (Basel, Switzerland)*, *24*(20), 3725. https://doi.org/10.3390/molecules24203725

Chipuk, J. E., Kuwana, T., Bouchier-Hayes, L., Droin, N. M., Newmeyer, D. D., Schuler, M., & Green, D. R. (2004). Direct activation of Bax by p53 mediates mitochondrial membrane permeabilization and apoptosis. *Science (New York, N.Y.)*, *303*(5660), 1010–1014. https://doi.org/10.1126/science.1092734

Committee on the State of the Science in Ovarian Cancer Research, Board on Health Care Services, Institute of Medicine, & National Academies of Sciences, Engineering, and Medicine. (2016). *Ovarian Cancers: Evolving Paradigms in Research and Care*. National Academies Press (US). Available from: https://pubmed.ncbi.nlm.nih.gov/27253000/

Constantinescu, T., & Lungu, C. N. (2021). Anticancer Activity of Natural and Synthetic Chalcones. *International journal of molecular sciences*, *22*(21), 11306. https://doi.org/10.3390/ijms222111306

Constantinescu, T., & Mihis, A. G. (2022). Two Important Anticancer Mechanisms of Natural and Synthetic Chalcones. *International journal of molecular sciences*, *23*(19), 11595. https://doi.org/10.3390/ijms231911595

De Zio, D., Cianfanelli, V., & Cecconi, F. (2013). New insights into the link between DNA damage and apoptosis. *Antioxidants & redox signaling*, *19*(6), 559–571. https://doi.org/10.1089/ars.2012.493

Debela, D. T., Muzazu, S. G., Heraro, K. D., Ndalama, M. T., Mesele, B. W., Haile, D. C., Kitui, S. K., & Manyazewal, T. (2021). New approaches and procedures for cancer treatment: Current perspectives. *SAGE open medicine*, *9*, 20503121211034366. https://doi.org/10.1177/20503121211034366

Dobbin, Z. C., & Landen, C. N. (2013). The importance of the PI3K/AKT/MTOR pathway in the progression of ovarian cancer. *International journal of molecular sciences*, *14*(4), 8213–8227. https://doi.org/10.3390/ijms140482132

Dudas, J., Ladanyi, A., Ingruber, J., Steinbichler, T. B., & Riechelmann, H. (2020). Epithelial to Mesenchymal Transition: A Mechanism that Fuels Cancer Radio/Chemoresistance. *Cells*, *9*(2), 428. https://doi.org/10.3390/cells9020428

Elmore S. (2007). Apoptosis: a review of programmed cell death. *Toxicologic pathology*, *35*(4), 495–516. https://doi.org/10.1080/01926230701320337

Fenwick, G. R., Lutomski, J., & Nieman, C. (1990). Liquorice, Glycyrrhiza glabra L.—Composition, uses and analysis. *Food Chemistry*, 38(2), 119–143. https://doi.org/10.1016/0308-8146(90)90159-2

Finucane, D. M., Bossy-Wetzel, E., Waterhouse, N. J., Cotter, T. G., & Green, D. R. (1999). Bax-induced caspase activation and apoptosis via cytochrome c release from mitochondria is inhibitable by Bcl-xL. *The Journal of biological chemistry*, *274*(4), 2225–2233. https://doi.org/10.1074/jbc.274.4.2225

Folsom, S. M., Berger, J., Soong, T. R., & Rangaswamy, B. (2023). Comprehensive Review of Serous Tumors of Tubo-Ovarian Origin: Clinical Behavior, Pathological Correlation, Current Molecular Updates, and Imaging Manifestations. *Current problems*

in diagnostic radiology, S0363-0188(23)00074-9. Advance online publication. https://doi.org/10.1067/j.cpradiol.2023.05.010

Franken, N. A., Rodermond, H. M., Stap, J., Haveman, J., & van Bree, C. (2006). Clonogenic assay of cells in vitro. *Nature protocols*, *1*(5), 2315–2319. https://doi.org/10.1038/nprot.2006.339

Gao, F., Huang, G., & Xiao, J. (2020). Chalcone hybrids as potential anticancer agents: Current development, mechanism of action, and structure-activity relationship. *Medicinal research reviews*, *40*(5), 2049–2084. https://doi.org/10.1002/med.21698

Gasparri, M. L., Bardhi, E., Ruscito, I., Papadia, A., Farooqi, A. A., Marchetti, C., Bogani, G., Ceccacci, I., Mueller, M. D., & Benedetti Panici, P. (2017). PI3K/AKT/mTOR Pathway in Ovarian Cancer Treatment: Are We on the Right Track?. *Geburtshilfe und Frauenheilkunde*, *77*(10), 1095–1103. https://doi.org/10.1055/s-0043-1189072

Gomes, M. N., Muratov, E. N., Pereira, M., Peixoto, J. C., Rosseto, L. P., Cravo, P. V. L., Andrade, C. H., & Neves, B. J. (2017). Chalcone Derivatives: Promising Starting Points for Drug Design. *Molecules (Basel, Switzerland)*, *22*(8), 1210. https://doi.org/10.3390/molecules22081210

Gravdal, K., Halvorsen, O. J., Haukaas, S. A., & Akslen, L. A. (2007). A switch from E-cadherin to N-cadherin expression indicates epithelial to mesenchymal transition and is of strong and independent importance for the progress of prostate cancer. *Clinical cancer research: an official journal of the American Association for Cancer Research*, *13*(23), 7003–7011. https://doi.org/10.1158/1078-0432.CCR-07-12632

Harish, V., Haque, E., Śmiech, M., Taniguchi, H., Jamieson, S., Tewari, D., & Bishayee, A. (2021). Xanthohumol for Human Malignancies: Chemistry, Pharmacokinetics and Molecular Targets. *International journal of molecular sciences*, *22*(9), 4478. https://doi.org/10.3390/ijms22094478

Hsu, Y. L., Chia, C. C., Chen, P. J., Huang, S. E., Huang, S. C., & Kuo, P. L. (2009). Shallot and licorice constituent isoliquiritigenin arrests cell cycle progression and induces apoptosis through the induction of ATM/p53 and initiation of the mitochondrial system in human cervical carcinoma HeLa cells. *Molecular nutrition & food research*, *53*(7), 826–835. https://doi.org/10.1002/mnfr.200800288

Huang, J., Chan, W. C., Ngai, C. H., Lok, V., Zhang, L., Lucero-Prisno, D. E., 3rd, Xu, W., Zheng, Z. J., Elcarte, E., Withers, M., Wong, M. C. S., & On Behalf Of Ncd Global Health Research Group Of Association Of Pacific Rim Universities Apru (2022). Worldwide Burden, Risk Factors, and Temporal Trends of Ovarian Cancer: A Global Study. *Cancers*, *14*(9), 2230. https://doi.org/10.3390/cancers14092230

Jandial, D. D., Blair, C. A., Zhang, S., Krill, L. S., Zhang, Y. B., & Zi, X. (2014). Molecular targeted approaches to cancer therapy and prevention using chalcones. *Current cancer drug targets*, *14*(2), 181–200. https://doi.org/10.2174/1568009614666140122160515

Jayson, G. C., Kohn, E. C., Kitchener, H. C., & Ledermann, J. A. (2014). Ovarian cancer. *Lancet (London, England)*, *384*(9951), 1376–1388. https://doi.org/10.1016/S0140-6736(13)62146-7

Kampan, N. C., Madondo, M. T., McNally, O. M., Quinn, M., & Plebanski, M. (2015). Paclitaxel and Its Evolving Role in the Management of Ovarian Cancer. *BioMed research international*, *2015*, 413076. https://doi.org/10.1155/2015/413076

Karthikeyan, C., Moorthy, N. S., Ramasamy, S., Vanam, U., Manivannan, E., Karunagaran, D., & Trivedi, P. (2015). Advances in chalcones with anticancer activities. *Recent patents on anti-cancer drug discovery*, *10*(1), 97–115. https://doi.org/10.2174/1574892809666140819153902

Kurman, R. J., & Shih, I.eM. (2016). The Dualistic Model of Ovarian Carcinogenesis: Revisited, Revised, and Expanded. *The American journal of pathology*, *186*(4), 733–747. https://doi.org/10.1016/j.ajpath.2015.11.011

Liu, G. H., Chen, T., Zhang, X., Ma, X. L., & Shi, H. S. (2022). Small molecule inhibitors targeting the cancers. *MedComm*, *3*(4), e181. https://doi.org/10.1002/mco2.181

Liu, J. F., Konstantinopoulos, P. A., & Matulonis, U. A. (2014). PARP inhibitors in ovarian cancer: current status and future promise. *Gynecologic oncology*, *133*(2), 362–369. https://doi.org/10.1016/j.ygyno.2014.02.039

Lord, C. J., & Ashworth, A. (2017). PARP inhibitors: Synthetic lethality in the clinic. *Science (New York, N.Y.)*, *355*(6330), 1152–1158. https://doi.org/10.1126/science.aam7344

Luyckx, M., Squifflet, J. L., Bruger, A. M., & Baurain, J. F. (2022). Recurrent High Grade Serous Ovarian Cancer Management. In S. Lele (Ed.), *Ovarian Cancer*. Exon Publications.

Maciejewska, N., Olszewski, M., Jurasz, J., Serocki, M., Dzierzynska, M., Cekala, K., Wieczerzak, E., & Baginski, M. (2022). Novel chalcone-derived pyrazoles as potential therapeutic agents for the treatment of non-small cell lung cancer. *Scientific reports*, *12*(1), 3703. https://doi.org/10.1038/s41598-022-07691-6

Matassov, D., Kagan, T., Leblanc, J., Sikorska, M., & Zakeri, Z. (2004). Measurement of apoptosis by DNA fragmentation. *Methods in molecular biology (Clifton, N.J.)*, *282*, 1–17. https://doi.org/10.1385/1-59259-812-9:001

Matos, M. J., Vazquez-Rodriguez, S., Uriarte, E., & Santana, L. (2015). Potential pharmacological uses of chalcones: a patent review (from June 2011 - 2014). *Expert opinion on therapeutic patents*, *25*(3), 351–366. https://doi.org/10.1517/13543776.2014.995627

Matthews, H. K., Bertoli, C., & de Bruin, R. A. M. (2022). Cell cycle control in cancer. *Nature reviews. Molecular cell biology*, *23*(1), 74–88. https://doi.org/10.1038/s41580-021-00404-3

Matulonis, U. A., Sood, A. K., Fallowfield, L., Howitt, B. E., Sehouli, J., & Karlan, B. Y. (2016). Ovarian cancer. *Nature reviews. Disease primers*, *2*, 16061. https://doi.org/10.1038/nrdp.2016.61

McIlwain, D. R., Berger, T., & Mak, T. W. (2013). Caspase functions in cell death and disease. *Cold Spring Harbor perspectives in biology*, *5*(4), a008656. https://doi.org/10.1101/cshperspect.a008656

Micalizzi, D. S., Farabaugh, S. M., & Ford, H. L. (2010). Epithelial-mesenchymal transition in cancer: parallels between normal development and tumor progression. *Journal of mammary gland biology and neoplasia*, *15*(2), 117–134. https://doi.org/10.1007/s10911-010-9178-9

Mirza, M. R., Monk, B. J., Herrstedt, J., Oza, A. M., Mahner, S., Redondo, A., Fabbro, M., Ledermann, J. A., Lorusso, D., Vergote, I., Ben-Baruch, N. E., Marth, C., Mądry, R., Christensen, R. D., Berek, J. S., Dørum, A., Tinker, A. V., du Bois, A., González-Martín, A., Follana, P., … ENGOT-OV16/NOVA Investigators (2016). Niraparib Maintenance Therapy in Platinum-Sensitive, Recurrent Ovarian Cancer. *The New England journal of medicine*, *375*(22), 2154–2164. https://doi.org/10.1056/NEJMoa1611310

Muñoz-Fontela, C., Mandinova, A., Aaronson, S. A., & Lee, S. W. (2016). Emerging roles of p53 and other tumour-suppressor genes in immune regulation. *Nature reviews. Immunology*, *16*(12), 741–750. https://doi.org/10.1038/nri.2016.99

Nakamura, K., Nakayama, K., Ishikawa, N., Ishikawa, M., Sultana, R., Kiyono, T., & Kyo, S. (2017). Reconstitution of high-grade serous ovarian carcinoma from primary fallopian tube secretory epithelial cells. *Oncotarget*, *9*(16), 12609–12619. https://doi.org/10.18632/oncotarget.23035

Naugler, W. E., & Karin, M. (2008). NF-kappaB and cancer-identifying targets and mechanisms. *Current opinion in genetics & development*, *18*(1), 19–26. https://doi.org/10.1016/j.gde.2008.01.020

Noser, A. A., Shehadi, I. A., Abdelmonsef, A. H., & Salem, M. M. (2022). Newly Synthesized Pyrazolinone Chalcones as Anticancer Agents via Inhibiting the PI3K/Akt/ERK1/2 Signaling Pathway. *ACS omega*, *7*(29), 25265–25277. https://doi.org/10.1021/acsomega.2c02181

Otto, T., & Sicinski, P. (2017). Cell cycle proteins as promising targets in cancer therapy. *Nature reviews. Cancer*, *17*(2), 93–115. https://doi.org/10.1038/nrc.2016.138

Ouyang, Y., Li, J., Chen, X., Fu, X., Sun, S., & Wu, Q. (2021). Chalcone Derivatives: Role in Anticancer Therapy. *Biomolecules*, *11*(6), 894. https://doi.org/10.3390/biom11060894

Ozaki, T., & Nakagawara, A. (2011). Role of p53 in Cell Death and Human Cancers. *Cancers*, *3*(1), 994–1013. https://doi.org/10.3390/cancers3010994

Padma V. V. (2015). An overview of targeted cancer therapy. *BioMedicine*, *5*(4), 19. https://doi.org/10.7603/s40681-015-0019-4

Plesca, D., Mazumder, S., & Almasan, A. (2008). DNA damage response and apoptosis. *Methods in enzymology*, *446*, 107–122. https://doi.org/10.1016/S0076-6879(08)01606-6

Podhorecka, M., Skladanowski, A., & Bozko, P. (2010). H2AX Phosphorylation: Its Role in DNA Damage Response and Cancer Therapy. *Journal of nucleic acids*, *2010*, 920161. https://doi.org/10.4061/2010/920161

Pujade-Lauraine, E., Hilpert, F., Weber, B., Reuss, A., Poveda, A., Kristensen, G., Sorio, R., Vergote, I., Witteveen, P., Bamias, A., Pereira, D., Wimberger, P., Oaknin, A., Mirza, M. R., Follana, P., Bollag, D., & Ray-Coquard, I. (2014). Bevacizumab combined with chemotherapy for platinum-resistant recurrent ovarian cancer: The AURELIA open-label randomized phase III trial. *Journal of clinical oncology: official journal of the American Society of Clinical Oncology*, *32*(13), 1302–1308. https://doi.org/10.1200/JCO.2013.51.4489

Qie, S., & Diehl, J. A. (2016). Cyclin D1, cancer progression, and opportunities in cancer treatment. *Journal of molecular medicine (Berlin, Germany)*, *94*(12), 1313–1326. https://doi.org/10.1007/s00109-016-1475-3e

Reuvers, T. G. A., Kanaar, R., & Nonnekens, J. (2020). DNA Damage-Inducing Anticancer Therapies: From Global to Precision Damage. *Cancers*, *12*(8), 2098. https://doi.org/10.3390/cancers12082098

Rozmer, Z., & Perjési, P. (2014). Naturally occurring chalcones and their biological activities. *Phytochemistry Reviews, 15* (1), 87–120. https://doi.org/10.1007/s11101-014-9387-8

Rudrapal, M., Khan, J., Dukhyil, A. A. B., Alarousy, R. M. I. I., Attah, E. I., Sharma, T., Khairnar, S. J., & Bendale, A. R. (2021). Chalcone Scaffolds, Bioprecursors of Flavonoids: Chemistry, Bioactivities, and Pharmacokinetics. *Molecules (Basel, Switzerland)*, *26*(23), 7177. https://doi.org/10.3390/molecules26237177

Sahin, I. D., Christodoulou, M. S., Guzelcan, E. A., Koyas, A., Karaca, C., Passarella, D., & Cetin-Atalay, R. (2020). A small library of chalcones induce liver cancer cell death through Akt phosphorylation inhibition. *Scientific reports*, *10*(1), 11814. https://doi.org/10.1038/s41598-020-68775-9

Saleh, A., & Perets, R. (2021). Mutated p53 in HGSC-From a Common Mutation to a Target for Therapy. *Cancers*, *13*(14), 3465. https://doi.org/10.3390/cancers13143465

Singh, N., Sarkar, J., Sashidhara, K. V., Ali, S., & Sinha, S. (2014). Anti-tumour activity of a novel coumarin-chalcone hybrid is mediated through intrinsic apoptotic pathway by inducing PUMA and altering Bax/Bcl-2 ratio. *Apoptosis: an international journal on programmed cell death*, *19*(6), 1017–1028. https://doi.org/10.1007/s10495-014-0975-2

Su, Y. K., Huang, W. C., Lee, W. H., Bamodu, O. A., Zucha, M. A., Astuti, I., Suwito, H., Yeh, C. T., & Lin, C. M. (2017). Methoxyphenyl chalcone sensitizes aggressive

epithelial cancer to cisplatin through apoptosis induction and cancer stem cell eradication. *Tumour biology: the journal of the International Society for Oncodevelopmental Biology and Medicine*, *39*(5), 1010428317691689. https://doi.org/10.1177/1010428317691689

Sun, G., Rong, D., Li, Z., Sun, G., Wu, F., Li, X., Cao, H., Cheng, Y., Tang, W., & Sun, Y. (2021). Role of Small Molecule Targeted Compounds in Cancer: Progress, Opportunities, and Challenges. *Frontiers in cell and developmental biology*, *9*, 694363. https://doi.org/10.3389/fcell.2021.694363

Sung, H., Ferlay, J., Siegel, R. L., Laversanne, M., Soerjomataram, I., Jemal, A., & Bray, F. (2021). Global Cancer Statistics 2020: GLOBOCAN Estimates of Incidence and Mortality Worldwide for 36 Cancers in 185 Countries. *CA: a cancer journal for clinicians*, *71*(3), 209–249. https://doi.org/10.3322/caac.21660

Vaughan, S., Coward, J. I., Bast, R. C., Jr, Berchuck, A., Berek, J. S., Brenton, J. D., Coukos, G., Crum, C. C., Drapkin, R., Etemadmoghadam, D., Friedlander, M., Gabra, H., Kaye, S. B., Lord, C. J., Lengyel, E., Levine, D. A., McNeish, I. A., Menon, U., Mills, G. B., Nephew, K. P., … Balkwill, F. R. (2011). Rethinking ovarian cancer: recommendations for improving outcomes. *Nature reviews. Cancer*, *11*(10), 719–725. https://doi.org/10.1038/nrc3144

Vermes, I., Haanen, C., Steffens-Nakken, H., & Reutelingsperger, C. (1995). A novel assay for apoptosis. Flow cytometric detection of phosphatidylserine expression on early apoptotic cells using fluorescein labelled Annexin V. *Journal of immunological methods*, *184*(1), 39–51. https://doi.org/10.1016/0022-1759(95)00072-i

Wang, C., & Youle, R. J. (2009). The role of mitochondria in apoptosis*. *Annual review of genetics*, *43*, 95–118. https://doi.org/10.1146/annurev-genet-102108-134850

Wang, G., Liu, W., Gong, Z., Huang, Y., Li, Y., & Peng, Z. (2020). Synthesis, biological evaluation, and molecular modelling of new naphthalene-chalcone derivatives as potential anticancer agents on MCF-7 breast cancer cells by targeting tubulin colchicine

binding site. *Journal of enzyme inhibition and medicinal chemistry*, *35*(1), 139–144. https://doi.org/10.1080/14756366.2019.1690479

Wang, K. L., Yu, Y. C., & Hsia, S. M. (2021). Perspectives on the Role of Isoliquiritigenin in Cancer. *Cancers*, *13*(1), 115. https://doi.org/10.3390/cancers13010115

Williams, A. B., & Schumacher, B. (2016). p53 in the DNA-Damage-Repair Process. *Cold Spring Harbor perspectives in medicine*, *6*(5), a026070. https://doi.org/10.1101/cshperspect.a026070

Wu, D., Li, Y., Zheng, L., Xiao, H., Ouyang, L., Wang, G., & Sun, Q. (2023). Small molecules targeting protein–protein interactions for cancer therapy. *Acta Pharmaceutica Sinica B.*https://doi.org/10.1016/j.apsb.2023.05.035

Yeung, T. L., Leung, C. S., Yip, K. P., Au Yeung, C. L., Wong, S. T., & Mok, S. C. (2015). Cellular and molecular processes in ovarian cancer metastasis. A Review in the Theme: Cell and Molecular Processes in Cancer Metastasis. *American journal of physiology. Cell physiology*, *309*(7), C444–C456. https://doi.org/10.1152/ajpcell.00188.2015

Yun, J. M., Kweon, M. H., Kwon, H., Hwang, J. K., & Mukhtar, H. (2006). Induction of apoptosis and cell cycle arrest by a chalcone panduratin A isolated from Kaempferia pandurata in androgen-independent human prostate cancer cells PC3 and DU145. *Carcinogenesis*, *27*(7), 1454–1464. https://doi.org/10.1093/carcin/bgi348

Zhang, S., Dolgalev, I., Zhang, T., Ran, H., Levine, D. A., & Neel, B. G. (2019). Both fallopian tube and ovarian surface epithelium are cells-of-origin for high-grade serous ovarian carcinoma. *Nature communications*, *10*(1), 5367. https://doi.org/10.1038/s41467-019-13116-2

Zhong, L., Li, Y., Xiong, L., Wang, W., Wu, M., Yuan, T., Yang, W., Tian, C., Miao, Z., Wang, T., & Yang, S. (2021). Small molecules in targeted cancer therapy: advances,

challenges, and future perspectives. *Signal transduction and targeted therapy*, *6*(1), 201. https://doi.org/10.1038/s41392-021-00572-w